ORIGINAL PAPER

Configuration planning for gaseous hydrogen refueling stations: a techno-economic assessment

Tjard Bätge[1] · Steffen Heinke[2] · Christian Weckenborg[3] · Marco Karig[1] · Wilhelm Tegethoff[2] · Jürgen Köhler[2] · Thomas S. Spengler[1]

© The Author(s) 2025

Abstract

Fuel cell electric heavy-duty trucks and the corresponding hydrogen refueling stations are part of policymakers' strategies to reduce road transport emissions. The construction of these refueling stations requires strategic planning on the configuration and, thus, the available capacity. No study in recent literature adequately considers the recovery process of gaseous hydrogen refueling stations between individual refueling events. By considering this recovery, this study systematically evaluates how random refueling demand profiles affect the thermodynamics and thereby the investment evaluation of differently configured stations. To this end, the underlying trade-off between high initial investment outlay and demand fulfillment as well as an ideal investment timing and potential future component upgrades are investigated. A simulation-based assessment and optimization approach is used. A thermodynamic model is developed to simulate discrete daily demand profiles. A mixed-integer linear program is developed to thereafter assess and optimize the configuration of the station's components. A comprehensive number of simulation runs in different market ramp-up scenarios for heavy-duty trucks build the data basis of the case study.

The configuration assessment shows that the stations' capability to perform back-to-back refueling significantly influences the investment valuation. Under-fulfillment of demand influences the valuation significantly more than differing electricity consumption. The results suggest aligning the configuration with the growing market share of the vehicles. Additionally, the investment timing should be postponed. These investment strategies are discussed from a technical design perspective. Finally, comprehensive sensitivity analyses are conducted, and the potential impact on other supply chain stakeholders is discussed.

Extended author information available on the last page of the article

Published online: 05 January 2026

🙼 Springer

1 Introduction

Fuel cell electric vehicles are being actively promoted by numerous laws and regulations, along with several other technologies, to reduce greenhouse gas emissions from road transportation. These regulations also aim to establish necessary initial hydrogen refueling station networks, thereby facilitating the adoption of the vehicles. The European Union, for example, adopted the alternative fuel infrastructure regulation in July 2023 (European Council 2023). Europe's main transport corridors must have hydrogen refueling stations in operation to serve heavy-duty trucks and passenger cars every 200 km and in all urban nodes by 2030, as mandated by this regulation.

There are different technological approaches to use hydrogen as fuel for road vehicles. Existing station concepts typically store hydrogen either in a liquid or in a gaseous state, and primarily dispense gaseous hydrogen at a pressure of either 350 or 700 bar to the vehicles (Bauer et al. 2019; Elgowainy et al. 2008). Each of these concepts poses high technical requirements on the design and operation of complex refueling systems. These requirements lead to high initial investment outlays (Reddi et al. 2017), therefore making the installation and design of these stations a long-term investment decision for potential operators (Forsberg and Karlström 2007).

The station design and, thus, the configuration of its components depends on several technical and economical considerations (Parks et al. 2020). Key influencing factors to choosing the configuration of the refueling components are the total demand, the variation in demand patterns, the installation as well as operation and maintenance costs, and the components' lifetimes, as summarized by Reddi et al. (2014). On the one hand, a well chosen configuration can reduce refueling costs (Reddi et al. 2014). One the other hand, the capacity of these components should also be matched with the demand and the variation of demand patterns (Tian et al. 2022). Particularly, the challenging situation, where multiple refueling events happen back-to-back and the refueling system might reach its technical limits, must be considered in the configuration planning (Elgowainy et al. 2008; Genovese et al. 2021). That is, this back-to-back refueling capability affects how variable refueling event patterns influence sales and, thus, the economic valuation of the refueling station. Thus, the long-term investment decision of designing and installing a hydrogen refueling station needs to consider the variable daily refueling patterns, as they affect both the future cash outflows and inflows.

Refueling demand is low and uncertain in the current early market stages (Kurtz et al. 2020; Forsberg and Karlström 2007). Thus, economically viable station design decisions should be based on a prediction of future demand (Kurtz et al. 2020). The investment valuation might benefit from expanding the capacity of the refueling station as the demand grows (Forsberg and Karlström 2007) or postponing the investment timing (Zhao and Liu 2023). The potential future component upgrade might also improve the station's capability to perform during demanding refueling patterns. These high frequency patterns occur rarely with low total demand in the beginning

and more often as demand grows. A sophisticated model is needed to systematically evaluate the technical and economical implications these variable refueling patterns have on the configuration decisions, potential component upgrades, and the investment timing.

This study contributes two main original aspects to the existing literature of hydrogen refueling station configuration planning. First, to the best of the authors' knowledge, this is the first study to comprehensively simulate changing, randomized daily demand profiles in a techno-economic assessment model to consider and systematically evaluate the thermodynamic effects of refueling event patterns on the investment evaluation of a hydrogen refueling station. This consideration requires not only initial investment outlays and variable cash outflows, which are commonly investigated, but also variable cash inflows to be evaluated in a strategic investment planning approach. In particular, the dependence of the investment evaluation on the stations' capability to perform demanding refueling patterns with multiple refuelings back-to-back is analyzed.

Second, building on this analysis, this study systematically investigates an ideal investment timing and potential future upgrades of components using mixed-integer linear programming. The case study depicts a 700 bar pipeline-supplied gaseous hydrogen heavy-duty truck refueling station. Comprehensive sensitivity analyses are conducted.

In the context of these contributions, this study answers the following research questions: How is the stations' capability to perform demanding refueling patterns related to its investment evaluation? What benefits are related to future upgrades of components considering the variability in demand? What benefits are related to a postponement of the investment considering the variability in demand?

The remainder of this study is structured in four sections: First, the necessary basics of current gaseous hydrogen refueling systems and their techno-economic assessment are introduced (Sect. 2). Second, the methodology used in this study is described (Sect. 3). Third, the results of a case study representing a gaseous hydrogen heavy-duty truck refueling station are presented (Sect. 4). Finally, the methods and findings are concluded, critically discussed, managerial implications are derived, and an outlook on potential future research is given (Sect. 5).

2 Technical background and literature review

In this section, the necessary basics of current gaseous hydrogen refueling stations and their techno-economic assessment is introduced. First, the technical operation principle and the effects of challenging refueling patterns on the thermodynamics and economics of the refueling system are discussed. Second, the existing literature on techno-economic assessments is reviewed.

2.1 Hydrogen refueling stations and back-to-back refueling

In contrast to conventional refueling stations, the refueling process with gaseous hydrogen is based on the pressure difference between the refueling station and the

vehicle tank. The vehicle tank is either filled directly by a compressor (known as "boosting") or from a high-pressure storage that was previously filled by a compressor (Mayer et al. 2019). A typical gaseous hydrogen refueling station with high-pressure storage consists of four main components as shown in Fig. 1. First, the *compressor* compresses the hydrogen from a lower pressure level supply source (e.g., a tube trailer or a pipeline with a buffer storage) to a higher pressure level, then the hydrogen is stored in the *high-pressure storage*. The storage typically consists of multiple individual banks (e.g., three or four), because of the energy savings compared to a single bank setup (Rothuizen and Rokni 2014). These banks might have different pressure levels and volumes (Blazquez-Diaz 2019; Caponi et al. 2022). The hydrogen heats up during the expansion into the vehicle tank (Elgowainy et al. 2017; Bauer et al. 2019). The heating of the gas is critical to the safety of the vehicle tank and must not exceed certain limits. Thus, the hydrogen is precooled by the *precooling unit* before it is released into the vehicle tank through the *dispenser* (Elgowainy et al. 2017; Bauer et al. 2019). The Society of Automobile Engineers (SAE) provides technical guidelines to the refueling process to ensure safe and convenient refueling processes for passenger cars and trucks (SAE International 2020, 2024). The guidelines determine the refueling process duration independently of station design (Caponi et al. 2022).

The economic design decisions of a gaseous hydrogen refueling station have to consider the interdependence of component characteristics such as compressor throughput and high-pressure storage size (Elgowainy et al. 2014). On the one hand, a bigger high-pressure storage size reduces the peak load of the compressor (Parks et al. 2020), and the storage size can be reduce with a greater compression capacity (Mayer et al. 2019). Initial investment outlays for the compressor and the storage module scale depending on their technical capacity. Initial investment outlays for the storage module are often assumed to scale degressively with pressure and linearly with volume, and compressor investments scale degressively with throughput or electrical power (Reddi et al. 2017; Mayer et al. 2019). That is, more storage capacity requires linearly more investment outlay, because the pressure is determined by the chosen technology. Stronger compressors, however, have a cost advantage over less powerful compressors. The implications of these different effects on dimensioning decisions are not trivial, because of the complex technical dependencies between the components. However, the scaling functions might favor large compressors with small storage if there is high demand. On the other hand, a lower pressure ratio between suction pressure and output pressure of the compressor reduces the electricity consumption (Mayer et al. 2019). Thus, high-pressure storage dimensioning
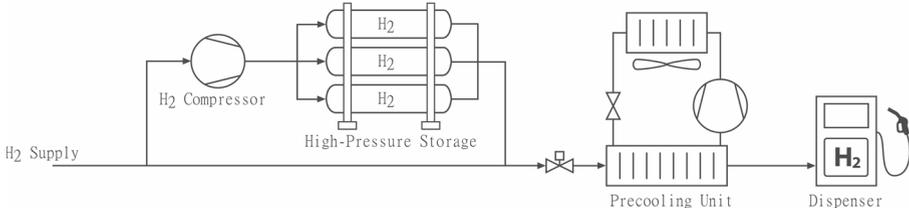
Fig. 1 General layout of a gaseous hydrogen refueling station

affects the compressor's electricity costs. Additionally, high-pressure storage dimensioning also has an impact on the energy consumption of the precooling unit (Bauer et al. 2019). Thus, the storage dimension is an important and complex design consideration from the economic perspective (Blazquez-Diaz 2019), and compressor and storage capacity should be economically balanced (Elgowainy et al. 2014).

The technical design and choice of the station's components aim to provide the customer with a refueling process in a reasonable time without exceeding any of the technical safety limits (Genovese et al. 2021). The peak hour presents the most challenging situation for the station with regard to maintaining temperature and pressure levels (Genovese et al. 2021). Therefore, many studies define the satisfaction of projected peak demand as a minimum design requirement for the station and its components, e.g. Mintz et al. (2009); Elgowainy et al. (2008, 2014, 2017); Parks et al. (2020); Ku et al. (2022) or Pratt et al. (2015). That is, the configuration of components is chosen in such way that the entire demand, particularly the maximum value during the peak hour, is fulfilled (Elgowainy et al. 2008). Thus, commonly used tools such as the hydrogen delivery scenario analysis model (HDSAM) also follow a peak demand design principle (Elgowainy et al. 2008; Mintz et al. 2009). These approaches therefore do not offer the possibility of deliberately designing a station below the peak value in order to achieve better overall capacity utilization. In general, a prediction of hourly demand profiles is the most relevant input to configuration and capacity models (Genovese et al. 2021).

Different measures are used to characterize the capability to handle the peak demand and to define the peak capacity, e.g. in H2 Mobility (2010). Our study adapts two main measures: the maximum number of vehicles per hour and the back-to-back capability. First, the *maximum number of vehicles per hour* is defined in this study as the maximum number of performed, standardized refuelings in one hour. The vehicle arrival times are assumed to be equally distributed over the hour. Second, the *back-to-back refueling capability* of a hydrogen refueling station is defined as the maximum number of back-to-back refueling events a refueling station can perform within the prescribed technical limits (cf. Elgowainy et al., 2017; Pratt et al., 2015; Reddi et al., 2014). To this end, the situation of back-to-back refueling is defined as standardized, consecutive refueling events with short lingering time between individual events (5 min for passenger cars) (Genovese et al. 2021). The components might not restore their previous state fully during the short idle times, e.g., fill level of the storage or temperature level of the precooling unit (Elgowainy et al. 2017; Genovese et al. 2021). This might lead to insufficient pressure and temperature levels to refuel following vehicles and, thus, to waiting times and a low utilization due to an unavailability of the station (Brown et al. 2012). Note, other definitions of back-to-back refueling capability exist or might be slightly different, e.g. in H2 Mobility (2010). Mayer et al. (2019) define the measure "long-term back-to-back capability" as the capability to refill the high-pressure storage completely and to the same condition as before previously to the next refueling event. Blazquez-Diaz (2019) uses a similar assumption.

Figure 2 illustrates an exemplary refueling pattern with three refuelings happening back-to-back. The shown station can only perform the first two refuelings without needing to additionally recover. The pressure levels of the station's high-pressure storage (consisting of three identical banks) are shown in blue, and the pressure level

of the vehicle tank is shown in red. The refueling is based on the pressure difference between the currently active bank and the vehicle tank. The compressor cannot fully recover all banks during the short time between the individual refueling events. During the refueling events, however, the compressor operates into the active bank (the one with the smallest positive pressure difference) assisting the refueling process not recovering the banks. The station, therefore, starts each process in a different initial state and finally fails to perform the third refueling. The third refueling is aborted (lightning symbol), before the pressure level of the fullest bank (dark blue line) drops below the pressure of the vehicle tank (red line). At this point, no positive pressure difference between any of the banks and the vehicle tank is achievable anymore. That is, this configuration has a back-to-back-capability of two as defined above. A more detailed description of the functionality of the station as well as the operation and switching logic of the components used in this study is given in Sect. 3.3.

The peak hour and the back-to-back refueling capability are not only of technical significance, but also have significant influence on the investment valuation of the system. The desired capability influences capacity as well as the initial investment outlays (Elgowainy et al. 2017). First, the corresponding under-fulfillment of demand due to the unavailability of the station causes variability in the sales cash flows dependent on demand profiles and station capability. Second, back-to-back fills require a large compressor and/or a large storage capacity (Reddi et al. 2014). Thus, highly back-to-back capable stations require large initial investment outlays. Therefore, the operator has to decide on the trade-off between high initial investment outlay and potential overcapacity, or low initial investment outlays and potential under-fulfillment of demand. Additionally, the variability in demand patterns and the design of the station interdependently affect energy consumptions of various components. These effects influence the variable operational cash outflow for electricity and, thus, the overall investment valuation.
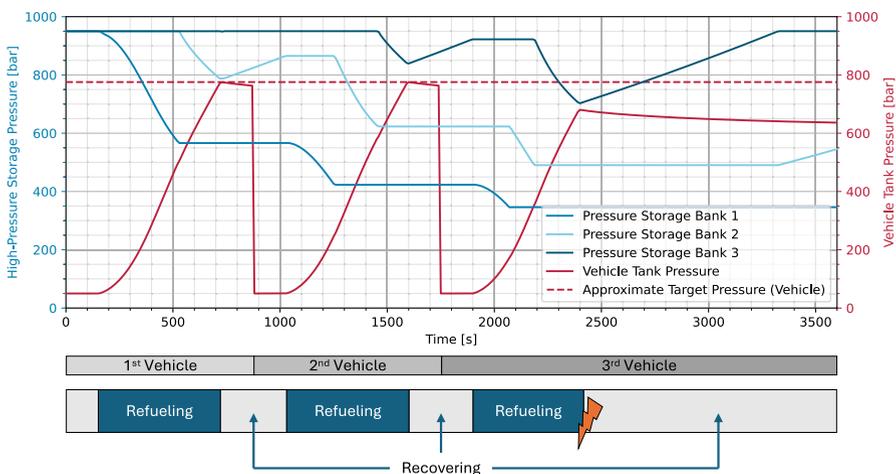
Fig. 2 Example for back-to-back refueling events (Back-to-Back Capability = 2)

A sophisticated model is needed to continuously simulate the different thermodynamic effects and complex interdependencies these variable refueling patterns and the station's back-to-back capability have on the investment valuation and the configuration decisions. As the development of the market is essential to the economic viability of these long-term decisions (Kurtz et al. 2020), the model must also enable the exploration of potential strategies for adapting the planning accordingly, such as investment postponement and component upgrades. To this end, the requirements for a suitable planning approach for the described problem can be summarized as follows:

(I)   Modeling of thermodynamic and technical interdependencies for multiple consecutive refueling events
(II) Incorporation of variable refueling demand patterns
(III) Use of a long-term, multi-period economic assessment method to assess absolute profitability with variable positive and negative monetary values
(IV) Modeling of flexible configuration decisions over time

The following section reviews current literature with regard to these requirements. Existing approaches are evaluated for their suitability to the described problem.

2.2 Existing literature on techno-economic assessments of hydrogen refueling stations

From a broad operations research and business economics perspective, the described problem of choosing a configuration of components over time determining the capacity of a technical system can be seen as a strategic capacity planning problem. Martínez-Costa et al. (2014) provide an overview of the development of capacity planning problems. In particular, this study's problem requires a decision on the expansion of capacity over time. The review by Luss (1982) summarizes the fundamentals of such capacity expansion problems. The classifications developed in both studies are used in later sections to structure this study.

There is extensive literature specifically on hydrogen refueling stations, which can be divided into three main categories. First, some studies take a technical focus on design decisions. Bauer et al. (2019) provide an overview over this literature stream. Second, some studies evaluate potential hydrogen refueling stations techno-economically at specific locations. Most of these studies include or focus on the decisions of hydrogen production equipment and use existing tools. Common tools are the HDSAM (Mintz et al. 2009) used to size hydrogen delivery pathways to minimize the levelized costs, the "Hybrid Optimization of Multiple Energy Resources" (HOMER) software (UL Solutions 2024) used to simulated and optimize for least-cost energy microgrids, and the "Hydrogen Station Capacity Evaluation" tool (HySCapE) (Sprik et al. 2018) used to simulate hydrogen refueling station configurations to estimate capacity. Al-Sharafi et al. (2024) provide a recent overview over this literature stream.

The third literature stream, which is the relevant stream to this study, includes novel, detailed modeling of components and interdependencies within the system, but also focus on their economic implications. Tian et al. (2022) provide a recent

overview of this stream. In the following, the analyzed literature is grouped into three subcategories: *design*-, *demand*-, and *investment*-focused studies. The studies are reviewed based on the requirements (I) to (IV) derived in the previous Sect. 2.1.

Multiple studies focus on the *design* and dimensioning of the components or investigate specific effects in the systems. Elgowainy et al. (2008) configure gaseous and liquid hydrogen refueling stations of different sizes from a cost perspective using HDSAM. The underlying demand profile in HDSAM and that study, the so-called "Chevron profile", is derived from real, conventional refueling data of the company Chevron (Elgowainy et al. 2008; Pratt et al. 2015). It is used in multiple subsequent studies. Mintz et al. (2009) also use HDSAM to configure a hydrogen refueling station based on peak demand comparing the Chevron profile with a flat profile with the same demand every hour of the day. The refueling costs are lower with the flat profile. Reddi et al. (2014) configure minimum cost gaseous hydrogen refuelings stations with HDSAM and investigate the trade-off between compression and storage capacity. High-pressure storage configurations are chosen with the objective to fulfill the most back-to-back refuelings for the Chevron profile. The technical report by Pratt et al. (2015) aims to provide reference designs using HDSAM to aid current and future operators. One criterion in the reference design is the possible number of back-to-back refuelings for the Chevron profile. Elgowainy et al. (2017) design the pre-cooling unit of a gaseous hydrogen refueling station to achieve minimum cost. One design criterion is the required number of possible back-to-back refuelings. Reddi et al. (2017) investigate the cost contributions of each component using HDSAM and the Chevron profile. Blazquez-Diaz (2019) focuses on the configuration of the high-pressure storage from a cost perspective. One underlying assumption in this study is a complete refill of the storage before the next refueling process, reducing the simulation need to a single refueling process. Mayer et al. (2019) conduct an economic assessment building on the technical consideration of the study by Bauer et al. (2019) in a two-study series. Different sized gaseous and liquid stations are configured based on the assumption of full recovery between refuelings (long-term back-to-back capability) similar to Blazquez-Diaz (2019). Different demands are scaled from the peak hour of the Chevron profile, and costs are analyzed. The strict long-term back-to-back capability assumption in Mayer et al. (2019) and Blazquez-Diaz (2019) cannot model the effects variable refueling patterns (II) might have on the investment valuation of the station, because the initial state of the station is restored before each refueling. However, Mayer et al. (2019) provide transparency on most of the underlying data. For these two reasons the study is used as a reference in this study. Caponi et al. (2022) techno-economically investigate the high-pressure storage with a focus on the difference of a single tank- and multiple tank-configuration. Caponi et al. (2022) scale the number of dispensers using the maximum number of vehicles in one hour. They consider the waiting time, but not the recovering of the station.

Multiple studies focus on understanding and modeling *demand* patterns for hydrogen refueling. Brown et al. (2012) quantitatively describe the effects of variable demand for an existing hydrogen refueling station. The study emphasizes the difference of average and maximum capacity using existing station data as an example. Nistor et al. (2016) develop a tool that stochastically generates refueling demand (II). The number of vehicles, arrival times, and the initial vehicle states are drawn from

probability distributions. Neither a long-term market development (III) nor investment and configuration decisions (IV) are considered. Grüger et al. (2018) stochastically model the refueling behavior of car-sharing collected by car-sharing companies and private passenger cars based on conventional refueling behaviour collected at two refueling stations. Subsequently, a hydrogen refueling station with on-site hydrogen production is scaled with an optimization model that minimizes the levelized costs of hydrogen. Investment strategies (IV) and back-to-back refueling effects (I) are not investigated. Genovese et al. (2021) analyze a data set of actual hydrogen refueling events with a special focus on back-to-back refuelings. It is concluded that future research should include back-to-back data in capacity planning, investigate the economic effects, and explore potential capacity upgrades according to demand. Sun et al. (2022) plan the capacity of a hydrogen refueling station using an optimization model based on a simulation of refueling behavior (II). Thermodynamic interdependencies (I) are not modeled. Šimunović et al. (2022) use a stochastic hourly demand profile (II) to account for customer behavior. Simulation series are performed to determine ranges for the sizing of components for different capacity levels. Investment strategies (IV) and back-to-back effects (I) are not considered.

Multiple studies focus on modeling the *investment* decisions in hydrogen refueling stations. Forsberg and Karlström (2007) investigate investment strategies (IV) for a refueling station that produces hydrogen on-site with an optimization model. In particular, the investment timing is analyzed using sensitivity analyses, and a potential future capacity upgrade is suggested. No back-to-back or detailed thermodynamic analyses (I) are performed. Zhao and Liu (2023) investigate the timing to invest in hydrogen refueling stations using real option analysis. Investments by a single firm and multiple firms cooperatively are considered. Zhao and Liu (2024) also investigate investment timing using real option analysis and dynamic programming. This study models future capacity upgrades (IV) as compound investments, and analyses different policy measures. Technical correlations (I) are not modeled in either study.

The results of the literature review are summarized in Table 1. It can be seen, that no single approach adequately models both the thermodynamic interdependencies for multiple consecutive refuelings (I) and the variable demand patterns (II). Additionally, no approach that models configuration decision over time (IV) considers thermodynamic interdependencies (I). A novel planning approach is developed in the following section to fill this research gap. This approach adapts ideas from the studies of Mayer et al. (2019); Grüger et al. (2018), and Forsberg and Karlström (2007), which all adequately model parts of the considered problem (see Table 1).

The predominantly used economic assessment method in the relevant literature is the levelized cost method (see Table 1). This method can be used to compare or rank alternative investment options with multi-period character (Short et al. 1995). However, this method only accounts for the negative monetary values (cash outflows or costs) and thus only partially fulfills the requirements of this study. Because potential demand nonfulfillment is investigated in this study, it is necessary to also consider positive monetary values (cash inflows or revenues) related to the varying sales to assess the absolute profitability of the investment and explore postponement strategies. To this end, this study uses the net present value method, which is widely used in theory and practice (Götze et al. 2015) and recommended for comparing mutually

Table 1 Classification of relevant literature

	Study	I Thermody-namics of consecutive refueling	II Variable demand profiles	III Long-term economic assessment	IV Configura-tion deci-sions over time	Economic assessment method[1]
Design-focused	Blazquez-Diaz (2019)	◐	○	◐	○	Total Cost
	Caponi et al. (2022)	◐	○	◐	○	CAPEX & OPEX
	Caponi et al. (2022)	◐	○	◐	○	LCOH
	Elgowainy et al. (2008)	●	○	◐	○	LCOH
	Elgowainy et al. (2017)	●	◐	◐	○	LCOH
	Mayer et al. (2019)	●	○	◐	○	Lifecycle Cost
	Mintz et al. (2009)	●	◐	◐	○	LCOH
	Parks et al. (2020)	●	○	◐	○	LCOH
	Pratt et al. (2015)	●	○	◐	○	LCOH
	Reddi et al. (2014)	●	○	◐	○	LCOH
	Reddi et al. (2017)	●	○	◐	○	LCOH
Demand-focused	Brown et al. (2012)	●	◐	○	○	–
	Grüger et al. (2018)	◐	●	◐	○	LCOH
	Nistor et al. (2016)	◐	●	◐	○	LCOH
	Šimunović et al. (2022)	◐	●	◐	○	LCOH
	Sun et al. (2022)	◐	●	◐	○	Total Cost
Investment-focused	Forsberg and Karlström (2007)	○	○	◐	●	Average Cost
	Zhao and Liu (2023)	○	○	●	◐	Real Op-tion (NPV)
	Zhao and Liu (2024)	○	○	●	◐	Real Op-tion (NPV)
	This Study	●	●	●	●	NPV

○ = requirement not fulfilled, ◐ = requirement partially fulfilled, ● = requirement fully fulfilled

(1) based on the wording of the respective authors

LCOH = levelized cost of hydrogen, NPV = net present value

exclusive investment alternatives (Short et al. 1995). This study follows the net present value formulation used in Götze et al. (2015).

3 Planning problem and modeling approach

In this section, first the configuration planning problem for a gaseous hydrogen refueling station is described. Second, the general assumptions are summarized. Third, the simulation-based optimization method, which consists of a thermodynamic model of the hydrogen refueling station and a mixed-integer linear program for the economic investment calculation, is introduced. Finally, the implementation is described briefly.

3.1 Problem description

The installation and design of a hydrogen refueling station is a long-term investment decision for a potential operator. The decision involves installing a specific configuration of components at each point in time t and operating $\boldsymbol{x}_t$ it accordingly (IV). The installation causes cash outflows $\boldsymbol{CF}_t^{\text{inst.}}$ equal to the initial investment outlays of the components. The operation causes cash outflows due to the necessary maintenance $\boldsymbol{CF}_t^{\text{maint.}}$ and net cash inflows $\boldsymbol{CF}_t^{\text{netsales}}$ resulting from the hydrogen sales and electricity consumption. Because these cash flows occur over a long time period, the investment is assessed using the net present value method (III).

The profiles of the demand significantly influence the design of the technical system in many different ways (see Sect. 2.1). Therefore, all technical dependencies must be considered in the investment decision (I). In the following, a detailed thermodynamic model that simulates a complete day of refueling is used for this. The variability between day-to-day demand patterns causes variable hydrogen mass flows and electricity consumption in the different components that translate to variable cash flows (II). For this reason, all variable cash flows need to be considered for the investment decision. The configuration of compressor and high-pressure storage size, in particular, influence the variable cash flows and, thus, decisions for their capacities $\boldsymbol{x}_{c,t}^{\text{comp.}}$ / $\boldsymbol{x}_{s,t}^{\text{stor.}}$ are necessary. To this end, the configuration choice and, thus, the installation of these two components $\boldsymbol{k}_{c,t}^{\text{comp.}}$ / $\boldsymbol{k}_{s,t}^{\text{stor.}}$ must be explicitly considered. The components' limited lifetime must also be considered. All other equipment (precooling unit, dispenser, and more) $\boldsymbol{k}_t^{\text{other}}$ can be aggregated into an additional component category, because these components are assumed to be designed for the maximum load occurring during a single refueling and, thus, are assumed to be identical for all configurations. The operator chooses the configuration of compressor c and high-pressure storage s in period t that maximizes the net present value of the investment.

Following the classification of Martínez-Costa et al. (2014), the described problem can be categorized as a single-site, capacity expansion and replacement problem. The replacement decision is necessary due to the components' limited lifetime and allows for a potential component upgrade. The problem includes two major decisions defined by Luss (1982): expansion sizes and expansion times.

3.2 Assumptions

The following general assumptions are made to model the real-world planning problem described above:

- All vehicles are homogeneous and refuel the same amount.
- Vehicles wait if they are currently connected to the station or are first in line and the maximum waiting time of this vehicle is not exceeded. A constant handling time is equally distributed before and after the actual refueling process.
- The vehicle arrival times are equally distributed within the hour, similar to, e.g., Elgowainy et al. (2017). Waiting may delay the start time of the refueling event.
- The hydrogen supply of the refueling station is not modeled in detail. An infinite source of hydrogen at constant pressure and ambient temperature is assumed (pipeline supply).
- The daily demand patterns are statistically independent, i.e. the nonfulfillment of demand on one day does not influence the demand (pattern) on following days.
- The lifetime of the components is considered. No liquidation values are considered, and the components can be dismantled without cost. All economic parameters are time-invariant.
- A deterministic optimization formulation is used. Uncertainties are considered using scenario and sensitivity analysis, and by considering the statistical moments of the net present value distribution (mean value, minimum, maximum, and confidence intervals) that result from the assumed randomness of the refueling demand profiles.

3.3 Modeling

The overall methodology consists of three parts. First, random demand profiles are generated for each scenario. Second, a thermodynamic model simulates 24 h of operation for each profile and each configuration of components. The simulation calculates how much demand can be fulfilled and how much electricity is consumed. The delivered hydrogen mass and the consumed electricity are stored to a database. Third, an economic model calculates the net present value based on these two quantities. The model is a mixed-integer linear program that is used to both assess certain configurations and to subsequently optimize the component capacities and investment timing. The overall methodology can be categorized as simulation-based optimization. Figure 3 provides a schematic overview of the coupling of methods.

3.3.1 Demand profile generation

The foundation for investigating the effects of refueling demand patterns on the economic valuation of a station are the refueling demand profiles (II). The underlying idea is similar to the study of Grüger et al. (2018), where refueling events are assigned to points in time based on time-resolved distributions borrowed from real data. Discrete random profiles are generated based on a given probability distribution of refueling events per hour. For a given number of vehicles, each refueling event is
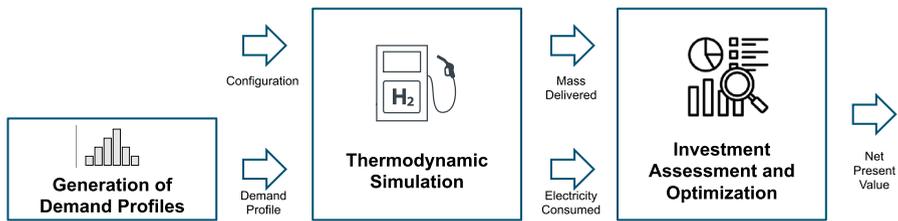
Fig. 3 Schematic overview of the simulation-based optimization approach
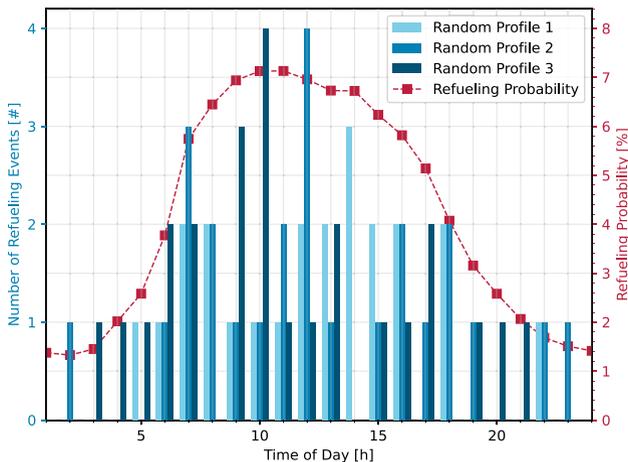

Fig. 4 Three random daily refueling patterns for 25 total vehicles and underlying probability distribution

assigned to a certain hour by the hour's probability. The sum of refueling events for each hour results in the pattern. Figure 4 illustrates three exemplary, random profiles with a total of 25 vehicles each as blue bar charts, and the underlying probability distribution with red markers. The random demand profiles represent the input to the thermodynamic simulation.

3.3.2 Thermodynamic simulation

A thermodynamic model is used to simulate the hydrogen refueling station (I). A schematic overview of the system model is shown in Fig. 5. The individual components are based on 0D and 1D methods. This means, that the thermodynamic balance equations are either averaged over the whole component (0D) or spatially discretized in one direction (1D), e.g., along the fluid flow. Similar 0D/1D models are used in the literature to thermodynamically simulate hydrogen refueling stations (e.g., Bauer et al. (2019) or Kuroki et al. (2021)). Typically, dynamic balance equations for mass and energy are used, while steady-state for the momentum balance is assumed. These balance equations are used to solve for the so-called state variables, such as pressure, specific enthalpy (or temperature), or density, as described in detail in Richter (2008). This approach allows the transient simulation of the hydrogen refueling station including the
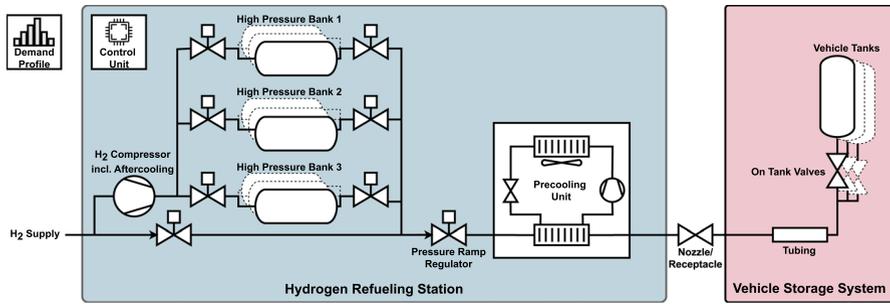
Fig. 5 Schematic overview of the thermodynamic model

vehicle storage system with a short computational time. The model is used to continuously simulate a full day with a corresponding demand profile for vehicle refueling. This means that both active refueling phases and non-refueling phases are included. During non-refueling phases, the station may perform recovery processes, if necessary, or remain idle. The relevant model outputs – the compressor and precooling unit power demand and the hydrogen mass flow rate transferred to the vehicle—are integrated over the whole day and used as inputs in the economic evaluation model. In the following, a general overview of the model structure and the implemented refueling logic is given. A detailed description of the relevant component models is given in Appendix A and the parametrization is summarized in Appendix Table 3.

The overall model is divided into three main parts: the vehicle storage system to be refueled, the hydrogen refueling station, and a simple waiting line model. The *vehicle storage system* consists of multiple, parallel tanks of Type IV (industrial classification scheme for hydrogen pressure vessels, summarized e.g. in Barthelemy et al. (2017)). Typically, all tanks in a vehicle behave similarly. Thus, only one tank is modeled in detail, and the result is upscaled to represent all parallel tanks. In addition, on-tank valves, tubing, and the receptacle are considered, resulting in pressure losses and thermal capacities. The vehicle storage system is connected to the hydrogen refueling station at the nozzle/receptacle interface, as in the real application.

The *hydrogen refueling station* considered in this work is composed of a hydrogen supply, a hydrogen compressor, multiple parallel high-pressure banks, a precooling unit, a pressure ramp regulator, and multiple valves. The hydrogen flows into the vehicle from one of the high-pressure banks, called the active pressure bank, due to a pressure difference to the vehicle. The number of parallel high-pressure banks is adjustable in the model. Research suggests the optimal number of banks to be three or four (Rothuizen and Rokni 2014). For this study it is fixed at three, similar to other studies (e.g., Talpacci et al. (2018) or Mayer et al. (2019)). The valve at the outlet of the active high-pressure bank is open, all other outlet valves are closed. The refueling is done with a constant average pressure ramp rate, similar to the SAE refueling protocols (SAE International 2020, 2024), which is controlled by the pressure ramp regulator. To allow fast refueling without overheating of the vehicle tanks, the precooling unit cools down the hydrogen flowing into the vehicle to a constant temperature. Details on the chosen pressure ramp rate and precooling temperature are given in Sect. 4.1. The high-pressure banks are refilled by the hydrogen compressor

from the hydrogen supply one by one. The inlet valve of the high-pressure bank being refilled is open, all other inlet valves are closed. Multiple strategies are plausible for choosing from which high-pressure bank to refuel the vehicle and especially for choosing which high-pressure bank to refill via the compressor at any given time. For this study, a strategy similar to Bauer et al. (2019) is chosen:

1. Vehicle refueling is done from the high-pressure bank with the lowest positive pressure difference relative to the vehicle. As the active buffer bank is being depleted, it is simultaneously being refilled by the hydrogen compressor. Typically, the depletion rate is higher, so the pressure in the bank drops as the vehicle pressure rises. If the vehicle tank's pressure is lower than the hydrogen supply's pressure, the vehicle is directly refilled from the hydrogen supply.
2. When the pressure difference becomes too low to maintain the desired average pressure ramp rate, the active bank is switched to the bank with the next lowest positive pressure difference relative to the vehicle. Refueling is then done from this newly active bank while it is being refilled by the compressor at the same time. Typically, this means that the high-pressure banks are active in the order of 1 to 3, if needed.
3. Refueling is finished once the vehicle storage system reaches a specified target state of charge. Refilling of the high-pressure banks now starts from the bank with the highest residual pressure level to the one with the lowest residual pressure level. Typically, this means from 3 to 1. The refilling of a high-pressure bank is finished once its nominal pressure level is reached.
4. In case no high-pressure bank with a positive pressure difference to the vehicle is left before the vehicle reaches its target state of charge, refueling is paused, and the high-pressure banks are refilled by the same logic as described under step 3. Once all high-pressure banks are refilled, the refueling of the vehicle resumes.
5. When a new vehicle arrives, refueling starts again at step 1, even if the refilling of the high-pressure banks is not yet finished and must be interrupted.

The *waiting line model* tracks the arrival times of vehicles at the refueling station based on the 24 h demand profile. If the dispenser is not occupied, arriving vehicles are directly connected to the refueling station to start the refueling process. If it is occupied and a vehicle is first in line, it will wait. If there is already another vehicle waiting in line or a maximum waiting time is exceeded, the vehicle is assumed to drive away, i.e., it will not be refueled. The maximum line length and maximum waiting time are adjustable in the model. Based on preliminary studies, it was determined that assuming any longer waiting line would only result in a marginally higher or equivalent economic valuation. If a vehicle is connected to the refueling station, it occupies the dispenser for the duration of the actual refueling process and the additional constant handling time.

The vehicle storage system model and the hydrogen refueling station model with a different parametrization have been validated using different experimental data, e.g., from De Miguel et al. (2016); Kuroki et al. (2018). Note, however, that in this study a generic parametrization is used to represent typical values for the investigated use case.

In addition to the simulation of the complete day, a reference case is simulated to illustrate the effects of back-to-back refuelings. The reference case is oriented at the assumption of Blazquez-Diaz (2019) and Mayer et al. (2019) that it is sufficient to simulate a single refueling process per configuration if the station is long-term back-to-back capable. That is, a single refueling is simulated per configuration and the required restoration time is determined. Hydrogen mass and electricity consumptions are then multiplied by the corresponding number of vehicles per hour, which is based on the required restoration time and a similar waiting logic as the full day simulation. This reference case does not consider the thermodynamic dependencies between components during consecutive refueling events.

3.3.3 Investment assessment and optimization

A mathematical optimization model is used to assesses the investment of certain configurations as well as the choice of economically optimal configurations and investment strategies (III). The objective of this model is to maximize the net present value by choosing which compressor and which high-pressure storage capacity to install in which planning period (IV). All technical dependencies are considered by using the results of the thermodynamic simulation as an input. Using the notation in Table 2, the model can be expressed as a mixed-integer linear program:

$$\max \text{NPV} = \sum_{t \in T} (\boldsymbol{CF}_t^{\text{netsales}} - \boldsymbol{CF}_t^{\text{inst.}} - \boldsymbol{CF}_t^{\text{maint.}}) \cdot (1+h)^{-t} \tag{1}$$

The objective function (1) represents the net present value as the discounted sum of the variable, net cash inflows from the sales of hydrogen $\boldsymbol{CF}_t^{\text{netsales}}$, the cash outflow related to the installation of components $\boldsymbol{CF}_t^{\text{inst.}}$, and the periodically recurring maintenance cash outflows $\boldsymbol{CF}_t^{\text{maint.}}$. The constraints to this optimization problem are grouped by their function.

$$\boldsymbol{CF}_t^{\text{netsales}} = \sum_{c \in C} \sum_{s \in S} (cf^{\text{H2}} \cdot m_{c,s,t} - cf^{\text{ele}} \cdot e_{c,s,t}) \cdot \boldsymbol{x}_{c,s,t} \; \forall t \in T \setminus \{0\} \tag{2}$$

$$\boldsymbol{CF}_t^{\text{inst.}} = (\sum_{c \in C} cf_c^{\text{constr.}} \cdot \boldsymbol{k}_{c,t}^{\text{comp.}} + \sum_{s \in S} cf_s^{\text{constr.}} \cdot \boldsymbol{k}_{s,t}^{\text{stor.}}$$
$$+ cf^{\text{other}} \cdot \boldsymbol{k}_t^{\text{other}}) \cdot (1 + f^{\text{surp.}}) \forall t \in T \tag{3}$$

$$\boldsymbol{CF}_t^{\text{maint.}} = \sum_{c \in C} cf_c^{\text{constr.}} \cdot \boldsymbol{x}_{c,t}^{\text{comp.}} \cdot f^{\text{maint., comp.}}$$
$$+ \sum_{s \in S} cf_s^{\text{constr.}} \cdot \boldsymbol{x}_{s,t}^{\text{stor.}} \cdot f^{\text{maint., stor.}}$$
$$+ \sum_{c \in C} \sum_{s \in S} cf^{\text{other}} \cdot \boldsymbol{x}_{c,s,t} \cdot f^{\text{maint., other}} \; \forall t \in T \tag{4}$$

Table 2 Notation investment assessment and configuration optimization

Sets	
$c \in C$	Set of compressors options
$(c, s) \in CS^{\mathrm{ex.}}$	Set of compressor and high-pressure storage configurations excluded from the optimization
$s \in S$	Set of high-pressure storage options
$t, t^{\mathrm{end}} \in T$	Set of all periods/years
Parameters	
$cf_c^{\mathrm{constr.}},$ $cf_s^{\mathrm{constr.}}$	Initial investment outlay of compressor c/storage s [€]
cf^{ele}	Purchase price of electricity [€/kWh]
cf^{H2}	Net margin on hydrogen [€/kg]
cf^{other}	Initial investment outlay of additional components [€]
$e_{c,s,t}$	Electricity consumed, if configuration (c, s) is used in period t [kWh]
$f^{\mathrm{maint.}}$	Maintenance rate [%]
$f^{\mathrm{surp.}}$	Surplus on investment [%]
h	Discount rate
$ls^{\mathrm{comp.}}, ls^{\mathrm{stor.}}$	Lifetime of compressor/high-pressure storage
$m_{c,s,t}$	Mass delivered, if configuration (c, s) is used in period t [kg]
Variables	
$\boldsymbol{CF}_t^{\mathrm{inst.}} \in \mathbb{R}_0^+$	Total cash flow corresp. to installation of all components in period t [€]
$\boldsymbol{CF}_t^{\mathrm{maint.}} \in \mathbb{R}_0^+$	Total cash flow corresp. to maintenance of all components in period t [€]
$\boldsymbol{CF}_t^{\mathrm{netsales}} \in \mathbb{R}_0^+$	Total net cash flow from hydrogen sales in period t [€]
$\boldsymbol{k}_{c,t}^{\mathrm{comp.}} \in \{0, 1\}$	Binary variable if compressor c is installed in period t
$\boldsymbol{k}_t^{\mathrm{other}} \in \{0, 1\}$	Binary variable if additional components are installed in period t
$\boldsymbol{k}_{s,t}^{\mathrm{stor.}} \in \{0, 1\}$	Binary variable if high-pressure storage s is installed in period t
$\boldsymbol{l}_{c,t}^{\mathrm{comp.}} \in \mathbb{R}_0^+$	Life of compressor c in period t
$\boldsymbol{l}_{s,t}^{\mathrm{stor.}} \in \mathbb{R}_0^+$	Life of high-pressure storage s in period t
$\boldsymbol{x}_{c,t}^{\mathrm{comp.}} \in \{0, 1\}$	Binary variable if compressor c is operated in period t
$\boldsymbol{x}_{c,s,t} \in \{0, 1\}$	Binary variable if configuration (c, s) is operated in period t
$\boldsymbol{x}_{s,t}^{\mathrm{stor.}} \in \{0, 1\}$	Binary variable if high-pressure storage s is operated in period t

Constraints (2)–(4) model the individual cash flows. The net sales $\boldsymbol{CF}_t^{\mathrm{netsales}}$ are calculated as the net margin (sales prices minus purchase price and taxes) of the delivered mass of hydrogen minus the cash flow for the consumed electricity, see Constraint (2). The cash flows are calculated by multiplying the results of the thermodynamic simulations ($m_{c,s,t}$, $e_{c,s,t}$) and the binary variable $\boldsymbol{x}_{c,s,t}$ that indicates whether a configuration with compressor c and storage s is operated in period t. The parameters $m_{c,s,t}$ and $e_{c,s,t}$ represent the mean values (or another statistical value) of the corresponding simulation results over the various random demand profiles. Each simulation result already takes into account the fulfillment of demand and the technical dependencies that lead to varying hydrogen mass and electricity consumption. The installation cash flows $\boldsymbol{CF}_t^{\mathrm{inst.}}$ are the sum over the installation cash flows

of compressor, storage, and other components, see Constraint (3). The installation cash flows are defined by the corresponding cash flow parameters multiplied by binary variables indicating whether the component is constructed in the corresponding period $k_{c,t}^{\text{comp.}}$/ $k_{s,t}^{\text{stor.}}$/ k_t^{other} and a surplus factor $f^{\text{surp.}}$ that accounts, among other things, for site preparation, engineering and design, and contingencies (see Pratt et al. (2015)). Constraint (4) defines the periodically recurring maintenance cash flow by a percentage $f^{\text{maint., comp.}}$/ $f^{\text{maint., stor.}}$/ $f^{\text{maint., other}}$ of the initial investment for the currently installed components.

$$\sum_{s \in S} \boldsymbol{x}_{c,s,t} \leq \boldsymbol{x}_{c,t}^{\text{comp.}} \ \forall c \in C, t \in T \tag{5}$$

$$\sum_{c \in C} \boldsymbol{x}_{c,s,t} \leq \boldsymbol{x}_{s,t}^{\text{stor.}} \ \forall s \in S, t \in T \tag{6}$$

$$\sum_{c \in C} \boldsymbol{x}_{c,t}^{\text{comp.}} \leq 1 \ \forall t \in T \tag{7}$$

$$\sum_{s \in S} \boldsymbol{x}_{s,t}^{\text{stor.}} \leq 1 \ \forall t \in T \tag{8}$$

$$\boldsymbol{k}_{c,t}^{\text{comp.}} \geq \boldsymbol{x}_{c,t+1}^{\text{comp.}} - \boldsymbol{x}_{c,t}^{\text{comp.}} \ \forall c \in C, t \in T \setminus \{t^{\text{end}}\} \tag{9}$$

$$\boldsymbol{k}_{s,t}^{\text{stor.}} \geq \boldsymbol{x}_{s,t+1}^{\text{stor.}} - \boldsymbol{x}_{s,t}^{\text{stor.}} \ \forall s \in S, t \in T \setminus \{t^{\text{end}}\} \tag{10}$$

$$\boldsymbol{k}_t^{\text{other}} \geq \sum_{c \in C}\sum_{s \in S} \boldsymbol{x}_{c,s,t+1} - \sum_{c \in C}\sum_{s \in S} \boldsymbol{x}_{c,s,t} \ \forall t \in T \setminus \{t^{\text{end}}\} \tag{11}$$

$$\boldsymbol{x}_{c,0}^{\text{comp.}} = 0 \ \forall c \in C \tag{12}$$

$$\boldsymbol{x}_{s,0}^{\text{stor.}} = 0 \ \forall s \in S \tag{13}$$

$$\boldsymbol{x}_{c,s,t} = 0 \ \forall (c,s) \in CS^{\text{ex.}}, t \in T \tag{14}$$

Constraints (5)–(14) model the configuration and logical relations between the components. A configuration (c,s) can be in operation ($\boldsymbol{x}_{c,s,t} = 1$) only if the corresponding compressor c and the corresponding high-pressure storage s are in operation $\boldsymbol{x}_{c,t}^{\text{comp.}}$/ $\boldsymbol{x}_{s,t}^{\text{stor.}}$ in the corresponding period t, see Constraints (5) & (6). Only one compressor out of the set of compressors C and one storage out of the set of storages S can be in operation at the same time, see Constraint (7) & (8). Constraints (9), (10), & (11) balance the operation and construction of compressor, storage, and other components respectively over the periods. Constraints (12) & (13) define an initially empty refueling system. Constraint (14) allows to exclude certain configurations

(c, s) from the decision space. For example, a planner might want to exclude all configurations with a back-to-back capability of less than a certain number of vehicles.

$$x_{c,t}^{\text{comp.}} \leq l_{c,t}^{\text{comp.}} \; \forall c \in C, t \in T \tag{15}$$

$$x_{s,t}^{\text{stor.}} \leq l_{s,t}^{\text{stor.}} \; \forall s \in S, t \in T \tag{16}$$

$$l_{c,t+1}^{\text{comp.}} \leq l_{c,t}^{\text{comp.}} - x_{c,t}^{\text{comp.}} + ls^{\text{comp.}} \cdot k_{c,t}^{\text{comp.}} \; \forall c \in C, t \in T \setminus \{t^{\text{end}}\} \tag{17}$$

$$l_{s,t+1}^{\text{stor.}} \leq l_{s,t}^{\text{stor.}} - x_{s,t}^{\text{stor.}} + ls^{\text{stor.}} \cdot k_{s,t}^{\text{stor.}} \; \forall s \in S, t \in T \setminus \{t^{\text{end}}\} \tag{18}$$

$$l_{c,t}^{\text{comp.}} \leq ls^{\text{comp.}} \; \forall c \in C, t \in T \tag{19}$$

$$l_{s,t}^{\text{stor.}} \leq ls^{\text{stor.}} \; \forall s \in S, t \in T \tag{20}$$

$$l_{c,0}^{\text{comp.}} = 0 \; \forall c \in C \tag{21}$$

$$l_{s,0}^{\text{stor.}} = 0 \; \forall s \in S \tag{22}$$

Constraints (15)–(22) model the life of the components $l_{c,t}^{\text{comp.}} / l_{s,t}^{\text{stor.}}$. Components can only be in operation if at least one period of life remains to the respective component, see Constraints (15) & (16). Constraints (17) & (18) balance the life of compressor and high-pressure storage over the periods. For this purpose, Constraints (19) & (20) ensure that the life cannot exceed the maximum lifetime of the respective component. Constraints (21) & (22) define the initial life to be zero. Additional restrictions can help to assess certain configurations without optimizing the choice of capacity size and timing, for example by enforcing that a specific component is constructed in a specific period. This principle was utilized to generate the results in Sects. 4.4 and 4.5.

$$CF_t^{\text{inst.}}, CF_t^{\text{maint.}}, CF_t^{\text{netsales}} \in \mathbb{R}_0^+ \; \forall t \in T \tag{23}$$

$$k_{c,t}^{\text{comp.}}, x_{c,t}^{\text{comp.}} \in \{0, 1\} \; \forall c \in C, t \in T \tag{24}$$

$$k_{s,t}^{\text{stor.}}, x_{s,t}^{\text{stor.}} \in \{0, 1\} \; \forall s \in S, t \in T \tag{25}$$

$$k_t^{\text{other}} \in \{0, 1\} \; \forall t \in T \tag{26}$$

$$l_{c,t}^{\text{comp.}} \in \mathbb{R}_0^+ \; \forall c \in C, t \in T \tag{27}$$

$$l_{s,t}^{\text{stor.}} \in \mathbb{R}_0^+ \; \forall s \in S, t \in T \tag{28}$$

$$x_{c,s,t} \in \{0, 1\} \; \forall c \in C, s \in S, t \in T \tag{29}$$

Constraints (23)–(29) define the domains of the variables. Given the domains of the variables and the characteristics of objective function and constraints, the presented economic model can be classified as a mixed-integer linear program.

3.4 Implementation

The different models of the simulation-based optimization approach are implemented in different software environments. The thermodynamic model is developed in Modelica, an object-oriented equation-based modeling language designed to model and simulate dynamic physical systems (Modelica Association 2023). The Dymola software (v2024x) from Dassault Systèmes (2023) is used as the modeling environment. The overall system model is composed of individual component models based on the software package TIL Suite from TLK-Thermo GmbH. (2024b), which includes, among others, the TIL model library for thermal components and systems and the TILMedia material data library. The resulting system of non-linear, hybrid differential-algebraic equations is solved numerically using the CVODE solver (Hindmarsh et al. 2005).

The generation of demand profiles and the economic assessment is implemented in Python (v3.10). The mixed-integer linear program is solved using Gurobi (v11) accessed through the Gurobi-Python-API. The thermodynamic Modelica model is exported to a Functional Mock-up Unit (FMU) according to the Functional Mock-up Interface standard (Modelica Association 2024). The FMU is simulated in Python using the Simulator Suite from TLK-Thermo GmbH (2024a), and the technical results are stored in Excel Files. In total, 2.4 Mio. daily thermodynamic simulations were computed in parallel on 60 threads on a machine with 56 cores Intel Xeon Platinum 8180 @2.50Ghz and 770 GB RAM in about 29 days. That is on average one day/demand profile is simulated per second when executed in parallel. The reference case (similar to Blazquez-Diaz (2019) and Mayer et al. (2019)), where individual refuelings are simulated and multiplied by the demand profile (see Sect. 3.3), was calculated in about 100 min (400 simulations per second). The mixed-integer program solves each scenario in about 0.05 s. Thus, the thermodynamic simulation represents the computational bottleneck for the developed approach.

4 Findings

In this section, the design of the case study is presented. Subsequently, the results of a techno-economic assessment of different configurations are described. For this purpose, first two illustrative configurations are compared both technically and economically. Second, the technical relationships are investigated in more detail. Third, the investments in the different configurations are evaluated in more detail. For this analysis, the investment is made in the first period and the components are replaced by identical components. Thus, expansion sizes and times are fixed. Fourth, the potential component upgrade strategy is analyzed by optimizing the component replacement and, thus, the expansion size only. Fifth, an additional, potential postponement strat-

egy is analyzed by optimizing the replacement and the timing. Finally, results from comprehensive sensitivity analyses are presented.

4.1 Case study design

The general setting of the case study is pipeline-supplied 700 bar gaseous hydrogen heavy-duty truck refueling. Truck refueling is generally characterized by larger refueling amounts and potentially back-to-back operation, and, thus, likely to be particularly demanding for the station (Ku et al. 2022). In particular, pipeline-supplied 700 bar refueling is energetically challenging and has not yet full technological readiness (Otto et al. 2024). At the same time, it is projected that there will be a significant focus on the 700 bar technology for future long-distance applications (European Commission 2025). Table 3 in the Appendix summaries all assumed parameters. The focus of this study is to compare different configurations and to illustrate the effects of the refueling patterns.

An uniform, standardized refueling is assumed. All trucks fill their 80 kg tank from initially 50 bar to 95 % final state of charge. The ambient temperature is 10 °C, which is the average ambient temperature in Germany (Mayer et al. 2019). The vehicle is refueled with a constant average pressure ramp rate similar to the SAE refueling protocols (SAE International 2020, 2024). Typically, in these protocols the average pressure ramp rate depends on the ambient temperature, initial filling level of the vehicle, and precooling temperature. In this case study, the ambient temperature and initial filling level are fixed at 10 °C and 50 bar, respectively. Thus, a fixed average pressure ramp rate of 7.75 MPa/min with a precooling temperature of -20 °C is chosen, based on the PRHYDE project (Ludwig-Bölkow-Systemtechnik GmbH 2023). This results in a refueling duration of approximately 9.5 min with a maximum refueling mass flow rate of 170 g/s and a tank temperature of 70 °C at the end of the fill. A handling time of 5 min is assumed, which is consistent with the back-to-back definition in Genovese et al. (2021). Thus, 4.14 refueling events are theoretically possible within one hour. The maximum waiting time is assumed to be 45 min, and the maximum waiting line length is assumed to be one vehicle.

As described in Sect. 3.1, the capacity of the compressor and the high-pressure storage are varied and optimized. The constant throughput/mass flow rate of the compressor (at a suction pressure of 80 bar) is varied in 30 kg/h steps in an interval of 30–300 kg/h. The total volume of the three banks is varied in 2 m^3 steps in an interval of 2–20 m^3. These capacities are chosen such that the booster-like concept (strongest compressor and smallest storage) can perform the standardized refueling because of the high throughput of the compressor, and the most buffer-like concepts (biggest storage volume and smallest compressor throughput) can perform the standardized refueling because of the amount of stored, previously compressed hydrogen. Both configurations achieve maximum back-to-back capability. All intermediate configurations balance the trade-off of compressor and storage capacity as described in Sect. 2.1. Each of the three storage banks has the same volume and same nominal working pressure of 950 bar.

The demand profiles are based on the average travel flow profile of the highway A2 near Hannover (Germany), which is one of Europe's most frequented highways

(Feder Highway Research Institute 2022). The market ramp-up is modeled as a general logistic function (S-curve similar to Forsberg and Karlström (2007)) representing the number of vehicles in each period (see Table 3). 20 Scenarios are modeled by varying the number of vehicles in the final period in 2.5 vehicles/day steps in an interval of 2.5 vehicles/day to 50 vehicles/day. That is, the station is on average fully utilized during the peak hour with the given daily profile in the most optimistic scenario (50 vehicles/day at one dispenser). Each year (365 days of operation) is represented by 60 randomly generated days, as described in Sect. 3.3.

The investment scaling functions used in Mayer et al. (2019), which in large part are based on Reddi et al. (2017), are utilized to model economies of scale for the investment in the components as described in Sect. 2.1. Currency and base year adjustments are made based on the DIN ISO 14008 norm (DIN 2020).

4.2 Illustrative examples

This section features a concise technical and economical comparison of two illustrative examples, before the later sections show detailed results. The two chosen configurations have similar investment outlays (2.42 Mio. € vs. 2.49 Mio. €), but differ significantly in terms of their technical characteristics. The "booster-like" configuration has the most powerful compressor in this case study with a throughput of 300 kg/h and a rather small storage with a total volume of 6 m^3. The other, "storage-focused" configuration has a storage with twice the total volume (12 m^3), but the least powerful compressor (30 kg/h).

Figure 6 shows the pressure levels of the stations and the vehicle tanks in an hour of back-to-back refueling for both configurations. The booster-like configuration (Fig. 6b) can perform all refuelings and thus achieves back-to-back capability over the complete day. The storage-focused configuration (Fig. 6a), however, has a back-to-back capability of two vehicles. The slopes of the storage pressure curves (blue) show that despite the smaller storage size the booster-like station depletes slower and also recovers faster due to the more powerful compressor. The refueling speed is identical for both stations, because the average pressure ramp rate is fixed (see red curve). In this illustrative comparison, the booster-like configuration would therefore be preferable from a technical perspective.

Figure 7 shows the investment evaluation of the two example configurations across the 20 different vehicle market scenarios. The scenarios are numbered in ascending order of maximum market share from 1 to 20. The error-bars show the mean net present value and the 95 % confidence interval. The background shading represents the range between the maximum and minimum values. The storage-focused configuration is advantageous relatively to the booster-like configuration in lower demand scenarios and disadvantageous in higher demand scenarios. The storage-focused configuration never achieves a positive mean net present value. The booster-like configuration, however, has a positive mean net present value in scenarios 10 to 20. The variability in net present value of the storage-focused configuration is significantly greater than the of the booster-like concept, because of the lower back-to-back capability. In this illustrative comparison, the more back-to-back capable, booster-like configuration is therefore also preferable from an economic perspective.
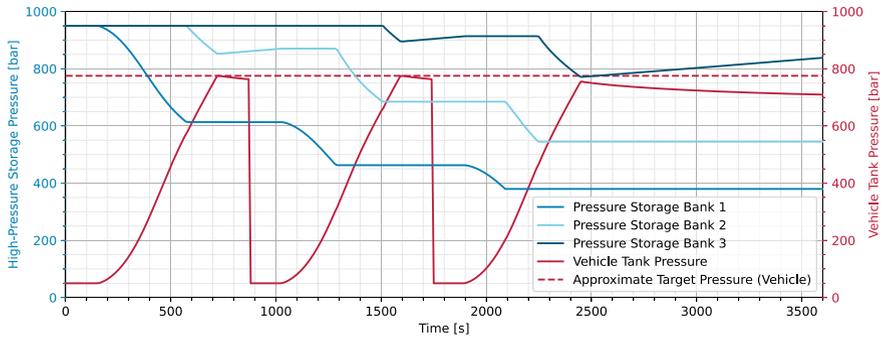
(a) "Storage-focused" Configuration
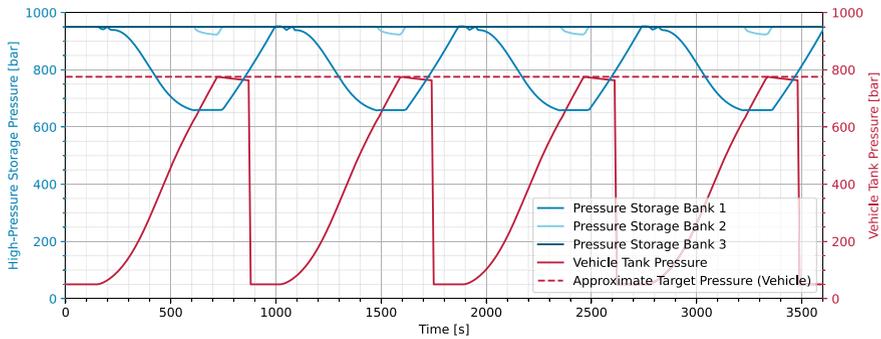
(b) "Booster-like" Configuration

Fig. 6 Pressure levels curves for two example configurations

More detailed analyses and explanations are provided for all 100 configuration in the following sections.

4.3 Results of the technical assessment

Two experiments were conducted for the technical assessment. The technical relationships of back-to-back refuelings are investigated for maximum capacity and peak hour capacity. First, each of the 100 configurations (10 compressor and 10 storage capacities) is loaded to maximum capacity. That is, refueling events happen back-to-back for 24 h. All configurations that can perform back-to-back all-day and, thus, have the highest possible capacity, are shown in the heat-maps of Fig. 8 below the black line. It is found that a higher compressor throughput and a larger high-pressure storage volume result in a greater maximum capacity, but the compressor size more significantly determines the capacity. For the given parametrization, a compressor with a flow rate of at least 270 kg/h is necessary for a station to be back-to-back-capable all-day even if the storage is twice the maximum size in this case study. Such a station has a maximum daily capacity of about 6.7 t/d for the given standardized refueling and waiting logic. The smallest station's maximum capacity is about 730 kg/d.
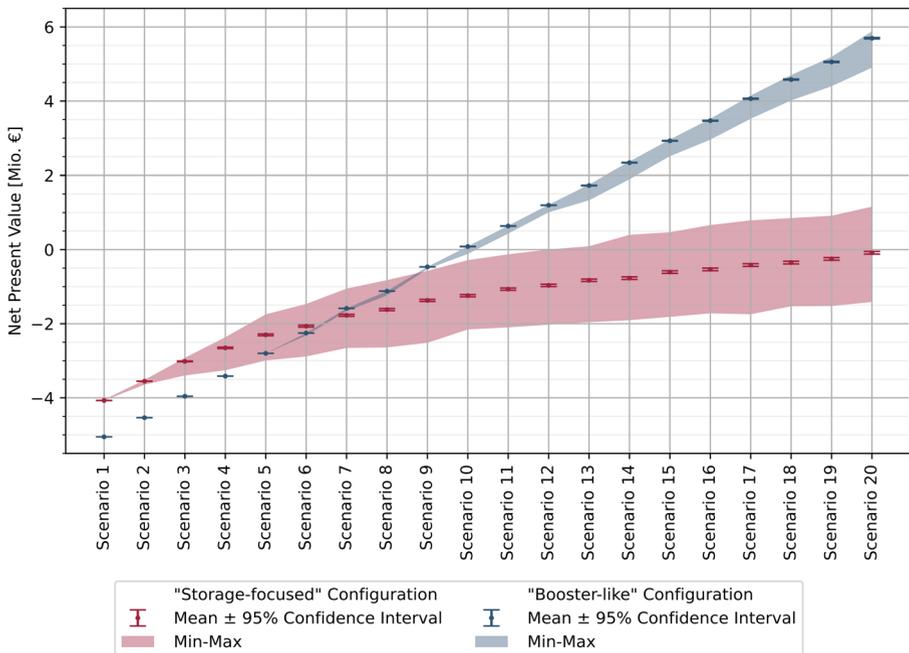
Fig. 7 Net present values for two example configurations across vehicle market scenarios (Min, Mean, Max, and 95 % Confidence Interval)

Second, series of one to five refuelings per hour are loaded on each configuration to determine the maximum number of vehicles per hour and the back-to-back capability as defined in Sect. 2.1. The vehicle arrival times in each series are equally distributed over the hour. Figure 8 compares the maximum number of vehicles per hour and the back-to-back capability of the different configurations. The difference of the measures is that in the first measure the vehicle arrival times are equally distributed over the hour, and in the second measure the refueling events happen back-to-back. Thus, the measures are identical for 5 refuelings per hour, because in this situation back-to-back refueling happens for the complete hour. This highest back-to-back capability value is achieved by 55 configurations. However, only the 12 configurations below the black line achieve back-to-back capability over the complete day. The maximum number of vehicles per hour and the back-to-back capability are found to show mostly similar assessments of the configurations. As expected, larger storage volumes and stronger compressors increase both measures. The influence of the compressor is more significant within the analyzed setting. There are 11 configurations that can perform more refuelings equally distributed than back-to-back. These configurations are less capital intensive than configurations that achieve identical assessment in both measures. Thus, considering these configurations in an early market with low initial utilization can be economically beneficial, because the peak hour of an early market might not involve extensive back-to-back refueling. For example, analyses in the following sections show that one of these configurations with a compressor with a throughput of 150 kg/h and a high-pressure storage with a total

(a) Max. no. Vehicles per Hour

(b) Back-to-Back Refueling Capability
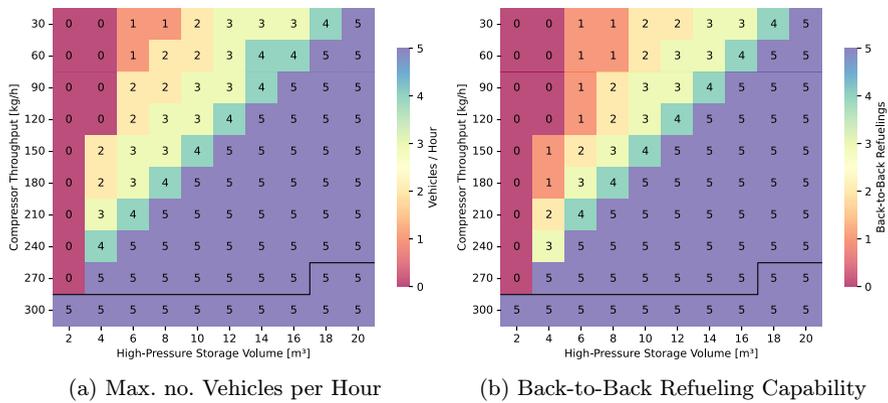
Fig. 8 Comparison of maximum number of vehicles per hour and back-to-back refueling capability

volume of 4 m³ represents the optimal solution to different scenarios. There are 13 configurations that cannot conduct at least one refueling process within the intended duration. These small configurations need to recover within the process to complete a single refueling process. Thus, these configurations are excluded in later considerations, because the duration is an important criterion for the customer's experience (Elgowainy et al. 2017).

The energy consumption during continuous refueling is determined by complex interdependencies as illustrated in Sect. 2.1. The electricity consumption of the compressor (1.67–1.93 kWh/kg$_{H2}$) is significantly higher than that of the precooling unit (0.07$-$0.09 kWh/kg$_{H2}$), which is consistent with other studies, e.g., Bauer et al. (2019) or Blazquez-Diaz (2019). For a single refueling process, electricity consumption is higher for larger compressor and storage capacities, but the storage size more significantly determines the electricity consumption. For all configurations that can perform back-to-back refueling for the complete hour, the specific electricity consumption of the precooling unit is on average about 7.5 % lower with five refuelings back-to-back than with a single refueling, and for the compressor on average about 6 % lower. This electricity consumption reduction results in an average of 0.018 €/kg$_{H2}$ electricity cost reduction during continuous refueling. However, the reduction is significantly higher for smaller compressors, where it can be about 12 % or 0.034 €/kg$_{H2}$, while the reduction for configurations with the largest compressor is only 0.16 to 0.30 % or 0.0005 to 0.0008 €/kg$_{H2}$. The reason is that these configurations with large compressor typically recover fully before the next refueling event.

4.4 Results of the investment assessment

The main experiment of the techno-economic assessment aims to analyze the economic impacts of varying refueling patterns for each of the 100 configurations across 20 vehicle market scenarios. Each scenario encompasses a 20-year planning horizon and includes 60 representative random daily demand profiles for each year. The scenarios are numbered in ascending order of maximum market share from 1 to 20. In the following, the results are focused on three scenarios (5, 10, and 15) that represent

a low, medium, and high demand scenario. The same underlying S-curve parameters are assumed, but the upper asymptote is varied (see Table 3). The demand in the last period for these scenarios is about 12.5 vehicles/day, 25 vehicles/day, and 37.5 vehicles/day, respectively.

Figure 9 illustrates the cash flows for the (150/4)-configuration, which consists of a compressor with a throughput of 150 kg/h and three high-pressure storage banks with a total volume of 4 m^3 over time in the medium demand scenario 10 (max. 25 vehicles/day). The bar charts represents the individual cash flow in that period and the red markers indicate the mean discounted cumulated cash flow as well as the minimum and maximum values. The variability results from variable delivered mass and consumed electricity for the 60 random profiles per year which translate into the variable net sales cash flows (green bars). The box-plots on the variable net sales cash flows show the distribution of these values. The variability in net sales cash flow increases as demand grows. The reason for the increasing variability is that with more vehicles over the day more profiles require extensive back-to-back refuelings. The station cannot perform all refuelings, and demand cannot be met while the station recovers. Changes in electricity consumption were found to have a significantly smaller effect than this under-fulfillment of demand. This finding appears consistent with other studies that revealed that the contribution from energy consumption is insignificant compared to the contribution of the initial investment outlays (Reddi et al. 2014).

Figure 10 shows the mean, minimum, and maximum net present values with a 95 % confidence interval for the mean value for exemplary configurations in the medium demand scenario. The curve patterns for the configurations not shown are similar and lie between those shown in terms of magnitude. The simulation for the full
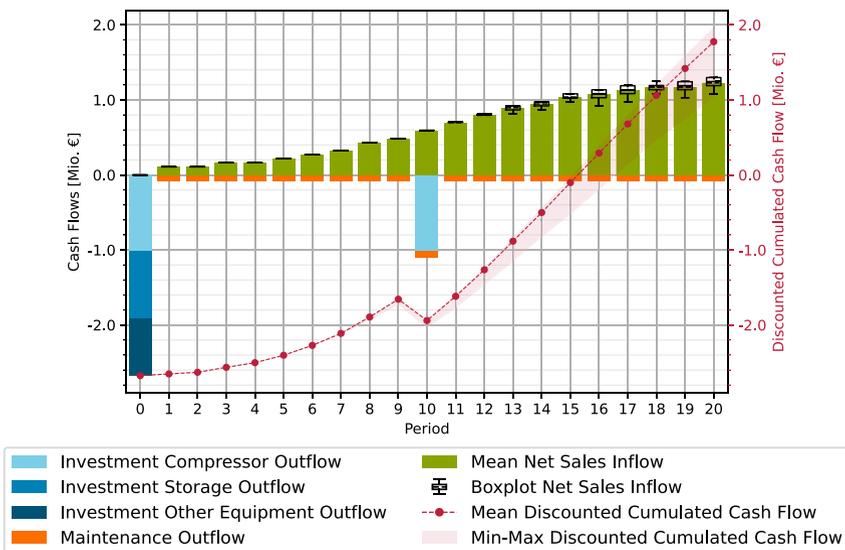

Fig. 9 Cash flows over time for the (150/4)-configuration in scenario 10

day is shown in red, and the reference case is shown in blue. The difference between the method is that the detailed simulation calculates continuous states between refueling events and allows a refueling to begin even if the station has not yet fully recovered from the previous refueling, while the reference case does not. A trade-off with compressor capacity can be found with both types of simulation. Compressors with a small throughput cannot fulfill all demand, and compressors with a higher throughput are more capital intensive. Thus, the highest net present value is achieved at an intermediate compressor capacity. The effect of demand under-fulfillment is also more significant than the increase in initial investment outlay. Additionally, the range of net present value distributions reduces with increasing compressor capacity because the under-fulfillment of demand shrinks. Compressors with higher throughput perform better during challenging demand patterns. The mean value is closer to the maximum for larger compressors, and the confidence interval is generally quite narrow compared to the range. This suggests that most days the total demand can be met when strong compressors are used. These effects can be seen in all scenarios but are more pronounced in the higher demand scenarios as demanding refueling patterns increase. No capacity trade-off can be found for the high-pressure storage. This means that greater storage volumes always reduce the economic valuation.

The net present value resulting from the reference case (blue) is in most cases lower than the net present value resulting from the detailed full day simulation method (red). Two effects cause the different valuation. First, more mass can be refueled to the customers in the detailed simulation (up to 35 % more mass in this scenario).
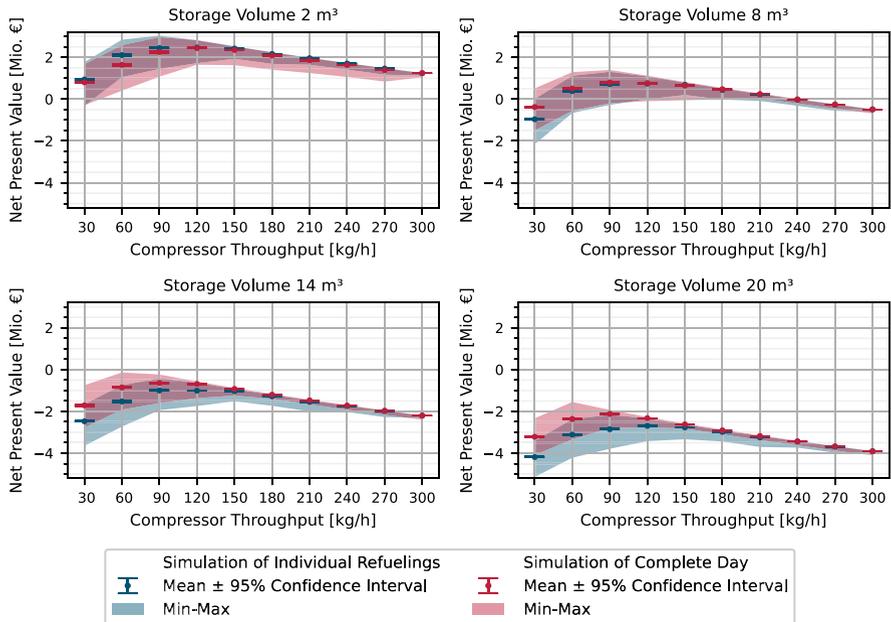
Fig. 10 Comparison of net present value between the single refueling simulation method and the complete day simulation method in the medium demand Scenario 10 (max. 25 Vehicles/Day) (Min, Mean, Max, and 95 % Confidence Interval)

This effect is particularly strong for small compressor throughput and rather large storage volume. Second, the lower average pressure level in the high-pressure banks results in a reduction of electricity consumption in the detailed simulation (up to 11 % less electricity per kg_{H2}). This effect is also particularly strong for small compressor throughput and rather large storage volume. With the assumed hydrogen margin and electricity prices, the first effect outweighs the second effect. For some configurations with rather small capacity, the reference case results in a higher net present value. The detailed simulation results in less refueled mass in these cases. This effect might be explained by an additionally necessary intermediate recovery and is more significant in higher demand scenarios. Thus, the economic evaluation is lower. It can be concluded that it is possible to model the most significant trade-off and effects using the reference method borrowed from existing literature. However, there is a systematic difference in the evaluation compared to the more detailed method, which might lead to overoptimistic evaluations of some configurations and too conservative evaluations of other configurations. Therefore, different configuration decisions in both, size and timing, are made in some scenarios, when using the reference case as the optimization's data basis. In the following sections, only the detailed simulation is used. This approach also offers the possibility for carrying out additional analyses with minimal changes to the model, e.g., for different control strategies, for multiple parallel refuelings, or for the usage of a thermal energy storage for the precooling unit. These investigations would require continuous modeling of the thermodynamic state variables between refueling events.

Figure 11 shows the mean net present values as a heat map, with the back-to-back capability of the station indicated by the digits on top for the low, medium, and high demand scenarios. The different scenarios have the highest net present value at different configurations. Compressors with small throughput are favorable for smaller demand. Moreover, smaller storage volumes tend to be favorable in all scenarios. This economic favorability is in a trade-off with the technical design decision. The highest theoretical net present values are with configurations that cannot refuel within the intended duration (back-to-back capability = 0) and should be excluded from the decision space. For example, in the low demand scenario no feasible configuration has a positive mean net present value. In the medium scenario, the feasible configuration with the highest mean net present value cannot refuel a second vehicle back-to-back. In the high demand scenario, the best configuration is, however, highly back-to-back-capable. Thus, the economically favorable configurations tend to become more back-to-back capable with higher demand scenarios. However, mainly stronger compressors are used to this end, but larger storage volumes are disadvantageous.

4.5 Results of the replacement optimization

The previous section has shown that different configurations are optimal with different demand scenarios and that variability increases over time but decreases with compressor throughput. A less capital intensive compressor could thus be advantageous in the first years, and a higher throughput compressor could reduce variability and improve mean net present value in the later years depending on the scenario.
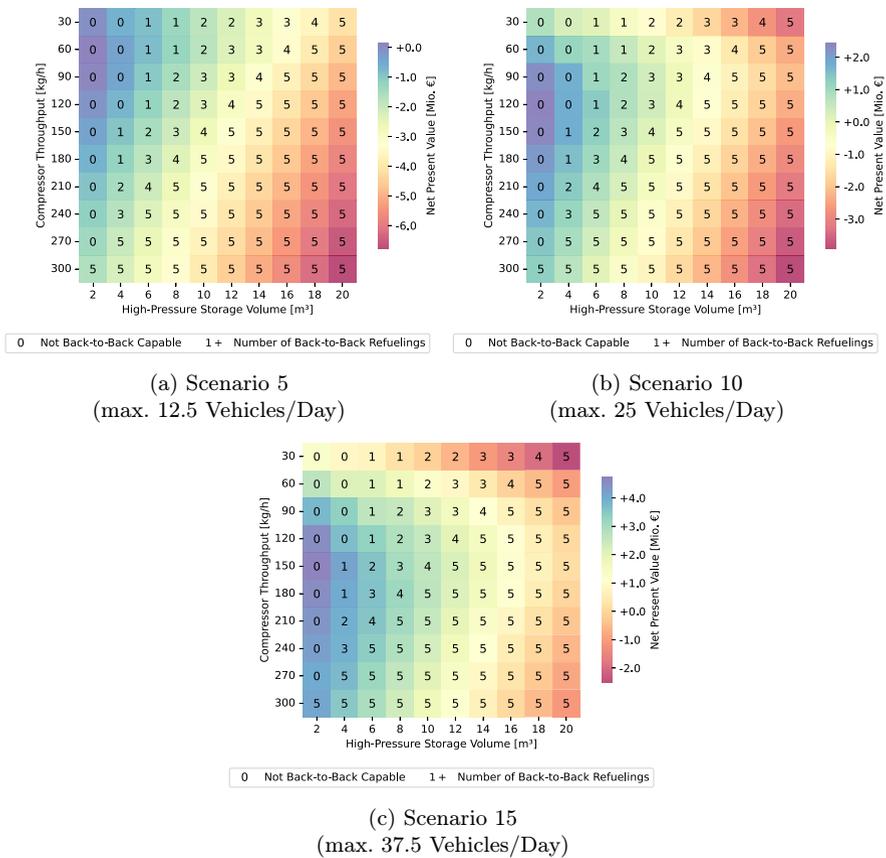
(a) Scenario 5
(max. 12.5 Vehicles/Day)

(b) Scenario 10
(max. 25 Vehicles/Day)

(c) Scenario 15
(max. 37.5 Vehicles/Day)

Fig. 11 Mean net present value and back-to-back capability of configurations

Thus, capacity upgrade over time, in particular for the compressor, might be advantageous. This strategy is analyzed using the mixed-integer program introduced in Sect. 3.3 with additional constraints to fix the investment timing. The mean mass delivered and mean electricity consumed are used, and thus the model optimizes for the mean net present value. All configurations that need an intermediate recovery to perform a single refueling are excluded. The replacement decision becomes necessary at the end of the component's life. Only the compressor is replaced during the planning horizon, because the assumed lifetime of the storage equals the planning horizon.

Figure 12 shows the cash flows for the optimal configurations for the high demand scenario with an identical compressor replacement (Fig. 12a) compared to an arbitrary compressor choice (Fig. 12b). The (150/4)-configuration is chosen when the replacement is fix, and the same configuration is chosen and then upgraded to a (270/4)-configuration when the arbitrary updates are allowed. That is, a not back-to-back capable configuration is chosen for this scenario when the compressor must be replaced with the identical component. This configuration, therefore, shows relatively high variability particularly in the second half of the planning horizon, which can be seen in the box-plots and the discounted cumulated cash flow range. When

the compressor can be upgraded, the same not back-to-back capable configuration is initially chosen, and then it is upgraded to a configuration with a back-to-back capability of five refuelings. This configuration uses a larger compressor throughput. The upgrade significantly reduces variability in net sales cash flows in the second half of the planning horizon, which can be seen in the box-plots after the replacement. The configuration with upgrade has an about 6 % higher mean net present value, and the dynamic payback period slightly lengthens, while the net present value range significantly decreases. The average utilization decreases about 9 %, but the average beta service level increases about 5 %. Similar results can be seen in most other scenarios. However, an upgrade is not beneficial for all scenarios. For example, the optimal configuration for the medium demand scenario is the (150/4)-configuration with and without upgrades allowed. For the low demand scenario, no suitable configuration has a positive mean net present value under the given parametrization. Thus, it is worth investigating if postponing the initial investment timing influences the valuation of a station in these scenarios.

4.6 Results of the replacement and timing optimization

This section investigates the strategy of postponing the investment. This analysis additionally allows the decision on the investment timing and thus the full flexibility of the model described in Sect. 3.3. That is, each type of compressor and storage can be constructed in any period. Thus, components can also be replaced by other components in any period considering the component's life. Additionally, the effects of different technical requirements on this strategy are investigated.

The initial investment timing is postponed for all scenarios with the given parametrization. Figure 13 shows the cash flows for the optimal solutions for the medium and high demand scenarios. The initial installation in the high demand scenario is postponed by three years. The postponement increases the mean net present value about another 7 % compared to previous analysis with just the component upgrade. The postponement by 6 years for the medium demand configuration results in an additional 31 % mean net present value increase. That is, the potential operators of hydrogen refueling stations should rather wait with an investment as it is significantly economically advantageous. The reason for this benefit is that the configuration can be better matched to the demand when not considering the low demand in early periods. However, this postponement must be seen as critical from a system's perspective as a delay in infrastructure ramp-up might delay the vehicle market ramp-up (chicken-egg problem). A delayed market ramp-up would, in return, change the planning basis for the infrastructure provider. The postponement might also effect up-stream supply chain stages because it causes planning uncertainty for the companies involved in hydrogen production and transport. Note that in scenarios 5–16 the compressor is replaced at the end of its lifetime. However, in scenarios 17–20 it is advantageous to replace the compressor up to two years before the end of its life. The storage is not replaced in any scenario.

Finally, the effect of excluding certain configurations based on the technical design decision to ensure a certain capability is investigated. To achieve this, the optimal configurations with a back-to-back capability of at least two (similar to
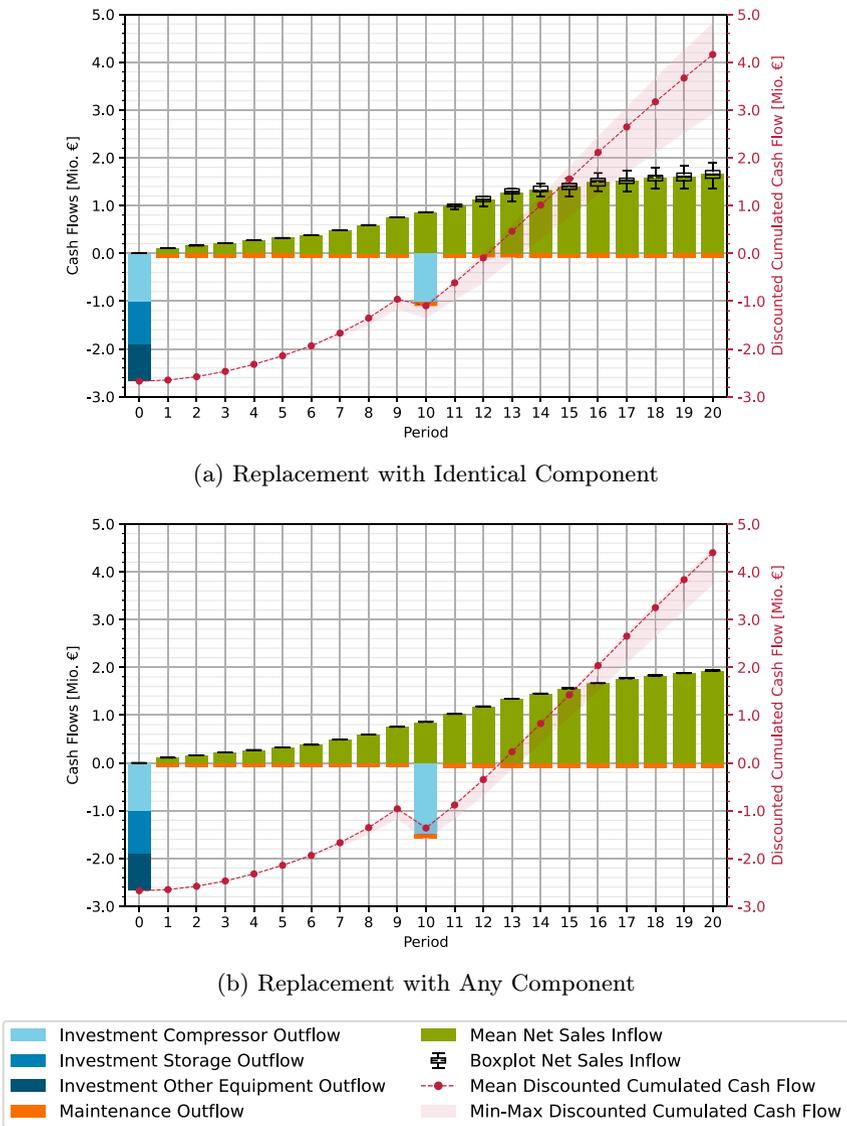
(a) Replacement with Identical Component

(b) Replacement with Any Component

Investment Compressor Outflow — Mean Net Sales Inflow
Investment Storage Outflow — Boxplot Net Sales Inflow
Investment Other Equipment Outflow — Mean Discounted Cumulated Cash Flow
Maintenance Outflow — Min-Max Discounted Cumulated Cash Flow

Fig. 12 Cash flows for optimal configurations in the high demand Scenario 15

the "medium size" in H2 Mobility (2010)) and the optimal configuration with a maximum number of vehicles per hour of at least one (all feasible configurations) are compared. Figure 14 shows the mean, minimum, and maximum net present values (Fig. 14a) and the period of initial investment (Fig. 14b) for the optimal investment strategy for each scenario. The differently colored lines represent the different minimum capability design requirements. That is, all other configurations with smaller capability were excluded from the corresponding optimization. There
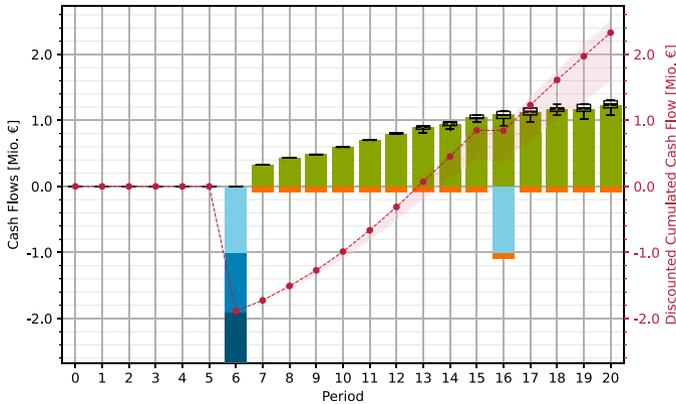
(a) Medium Demand Scenario 10
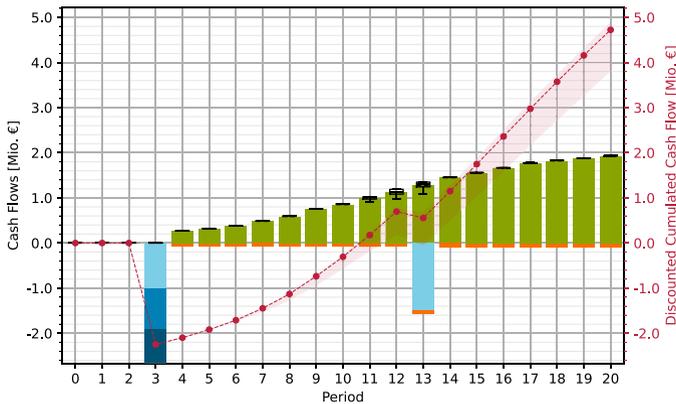
(b) High Demand Scenario 15

Fig. 13 Cash flows over time for optimal configurations with postponement

is a relatively small difference in net present values and a bigger difference in initial investment periods between the two requirements. As expected, the less strict requirement results in slightly higher net present values and earlier investments. Additionally, net present value variability increases significantly. There exists a trade-off between a slightly higher net present value and a significantly higher variability of the investment assessment when the technical requirement is defined less strictly. Note that the solution with a back-to-back capability of at least two is the (300/2)-configuration for all scenarios, which is the most booster-like configuration and back-to-back capable for the complete day. Any stricter requirement would result in the same solution.

4.7 Sensitivity analyses

This section comprehensively checks assumptions of the previous results. First, the technical assumptions of identical nominal working pressures for the high-pressure storage and 80 bar suction pressure for the compressor are validated. Second, the sensitivity of the economic parameters are analyzed. Finally, the solutions of the deterministic optimization are checked in other scenarios.

Identical nominal working pressure to all banks of the high-pressure storage are assumed in this study. Typically, different pressure levels for the banks are assumed in the literature to reduce the average pressure ratio and, thus, electricity consumption
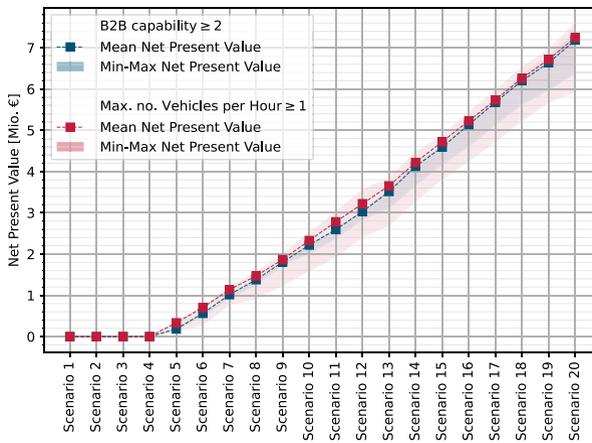
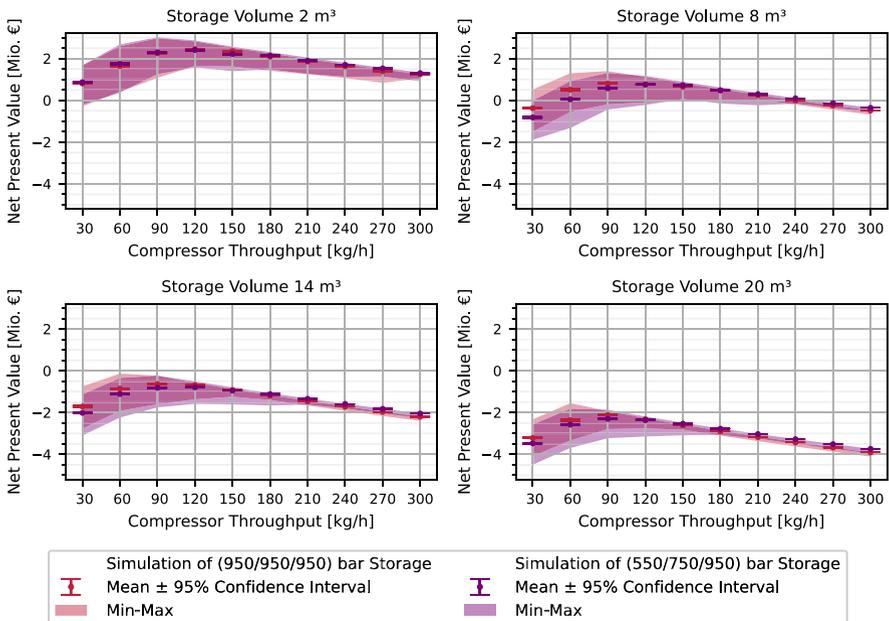(a) Mean, Min., & Max. Net Present Value
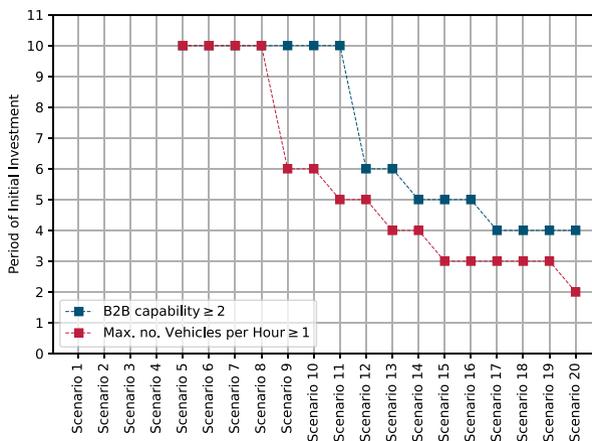
(b) Period of Initial Investment

Fig. 14 Comparing optimal configurations for different back-to-back requirements

(Caponi et al. 2022). That is why a setup with a 550 bar, a 750 bar, a 950 bar pressure level for the three identical banks was tested and compared to the basis case with three 950 bar tanks. Figure 15 shows the economic result of this comparison for the medium demand scenario. Similar mean net present values are found for the different setups. The trade-offs described above are also found with different pressure levels. For smaller storage volumes and/or strong compressors, staggered pressures seem slightly advantageous, probably because of the faster restoration. For large storage volumes and/or small compressors, identical pressures are advantageous. The result indicate that future research could extend this study and systematically investigate the influence of different pressure levels on the capability to perform back-to-back refueling.

This study also assumed 80 bar suction pressure for the compressor. This assumption represents approximately a direct connection to a potential future main "backbone" pipeline, while 20 bar approximately represents a connection to a local distribution pipeline (NOW GmbH 2024). Figure 16 shows the economic result of this comparison for the medium demand scenario. The reduction in supplied pressure significantly reduces the economic valuation for two reasons. First, significantly more electric energy is required for the refueling process with the greater pressure ratio. Second, stronger and, thus, more capital intensive compressors are necessary, because the flow rate correlates approximately linearly to the suction pressure (Elgowainy et al. 2014). A throughput factor is used to adjust the necessary investment outlay of the compressor to the associated suction pres-

Fig. 15 Comparison of net present values between high-pressure storage with identical vs. staggered pressure levels in the medium demand scenario (Min, Mean, Max, and 95 % Confidence Interval)

sure (see Table 3). For the given parametrization, no configuration is profitable in the medium demand scenario, when assuming 20 bar suction pressure c.p. By further varying the suction pressure, it is found that a minimum pressure of about 40 bar is needed for a feasible configuration with a positive net present value in this setting. About 50 bar suction pressure is needed for a profitable station with a minimum back-to-back capability of two. That is, the profitability of a pipeline-supplied heavy duty 700 bar hydrogen refueling station is significantly sensitive to the pipeline pressure and, thus, the location. This finding is consistent with NOW GmbH (2024).

Various economic parameters, which are summarized in Table 3 in the appendix, are assumed in this study. Figure 17 shows the influence of a change in different parameters c.p. on the mean net present value of the optimal configuration for the medium demand scenario. A back-to-back capability of at least two vehicles is assumed. The net margin on hydrogen exhibits the greatest sensitivity on the economic valuation. The effect is over-proportional and approximately linear. This means that a change in margin results in a more pronounced change in mean net present value, e.g., a reduction of 10 % decreases the mean net present value by about 20 %. This finding is particularly important to operators because this study assumes rather optimistic sales margins and quantities (each refueling from 50 bars to 95 % state of charge). Additionally, this value can be influenced by the operator. The discount rate assumed by the operator exhibits the second biggest effect. The initial investment outlays are varied for all components uniformly.
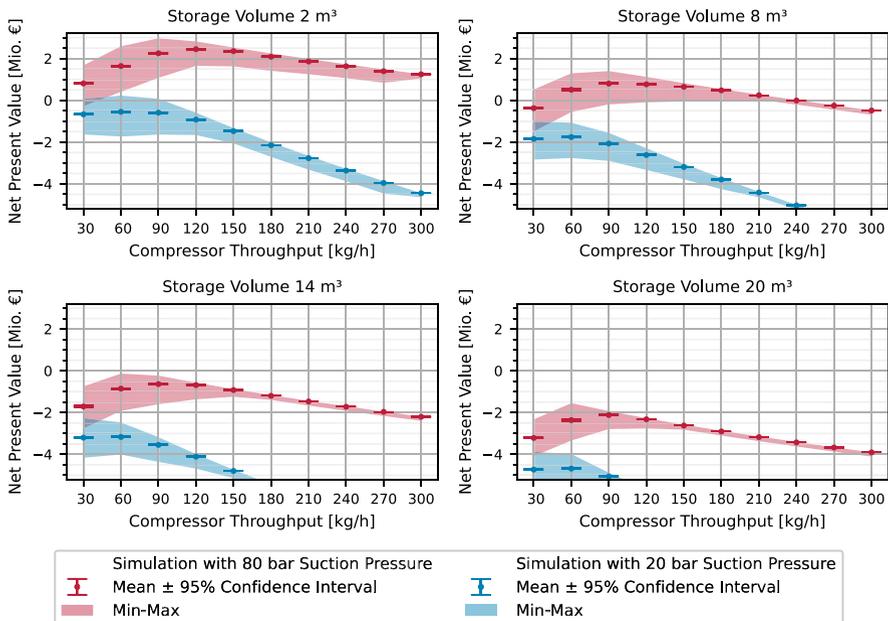
Fig. 16 Comparison of net present values between 80 bar vs. 20 bar suction pressure in the medium demand scenario (Min, Mean, Max, and 95 % Confidence Interval)

The sensitivity of the outlays is the third highest out of the analyzed parameters, i.e. the determination of component prices and the choice of the component supplier should be prioritized. Additionally, the throughput factor and the compressor lifetime appear to be very sensitive. This throughput factor relates the price of the compressor to the suction pressure. Thus, particularly the compressor choice should be an important criterion to the planner. Note that the stepwise relationship of the lifetime results from the discrete planning periods. The other sensitivities are relatively small.

Deterministically-known vehicle market ramp-ups are assumed in this study. However, this forecast might be uncertain in real planning. Figure 14a shows the range of mean net present values when assuming different scenarios. It has also been found that the valuation of configuration within the same scenario varies significantly, and different configurations were advantageous for different scenarios (see Fig. 11). Thus, it is necessary to investigate how the optimal decisions would perform in the other scenarios for which the decisions were not optimized. Figure 18 shows the range between the minimum and maximum payoff (mean net present value) that each of the 20 decisions can achieve. Figure 18a shows the optimizations over all feasible configurations (maximum number of vehicles per hour ≥ 1) and Fig. 18b shows the optimization over only the back-to-back capable stations (back-to-back capability ≥ 2). Each decision is optimized for one scenario, and the corresponding objective value is shown (blue square). Additionally, the worst regret for each decision is shown (red). It can be seen that
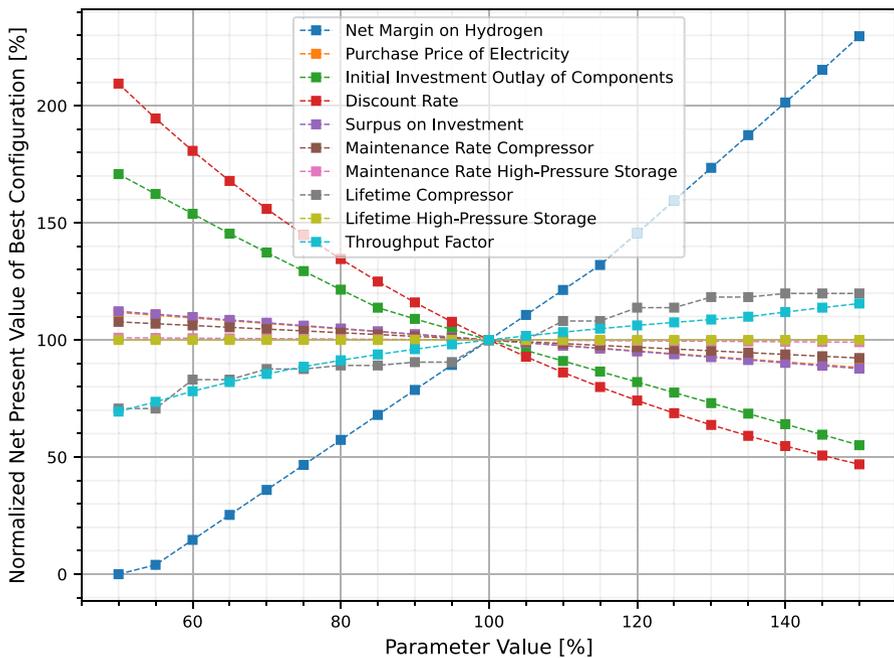

Fig. 17 Sensitivity analysis on economic parameters

the valuation of the investment in both cases is highly sensitive to the vehicle market scenario. But the optimal decisions for different scenarios are quite similar. That is why the ranges of possible payoff for the different configurations are similar. A relatively good payoff can be achieved even if the decision making was based on a wrongly assumed scenario. For the case with the back-to-back capable design requirement (Fig. 18b) there are only five different optimal decisions for the 20 scenarios: one for scenarios 1–4, 5–11, 12–13, 14–16, and 17–20. These only differ in the investment timing, but not in the chosen configuration. The optimal decisions where back-to-back refueling is not required (Fig. 18a) are
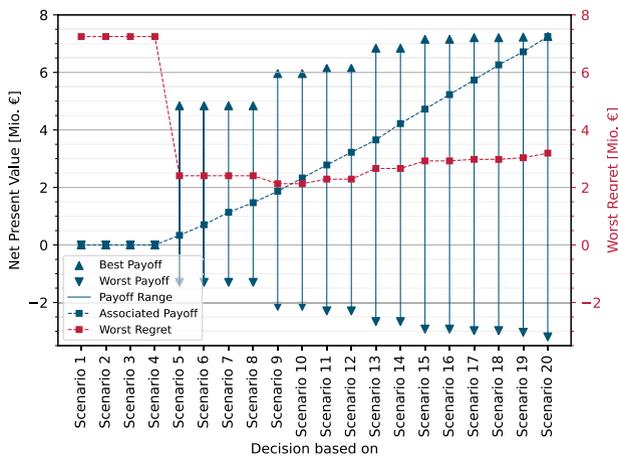
(a) Max. No. Vehicles per Hour ≥ 1
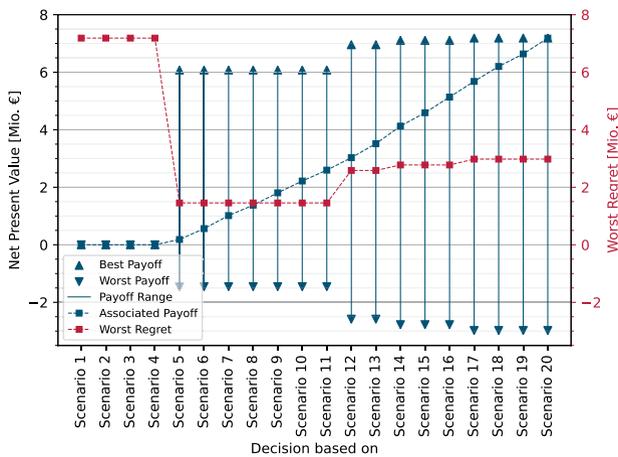
(b) Back-to-back Capability ≥ 2

Fig. 18 Performance of optimal configurations in other scenarios

more adapted to the associated scenario, i.e. more different decisions, which also structurally differ, are optimal for the different scenarios because the capability assumption is less strict. The decisions therefore cannot perform as well if a better scenario occurs (lower best payoff), but do not perform as badly if a worse scenario occurs (higher worst payoff). A decision maker acting on a min-max criterion would not open a station for the given parametrization, and a decision maker with a min-max-regret approach would base the decision on the scenarios 9 or 10 independently of the back-to-back requirement. In summary, the absolute evaluation is highly sensitive to an accurate prediction of the total demand, but the decisions, particularly if back-to-back refueling capability is required, appear rather robust. A possible approach to predict more accurate total demand ramp-ups could be to cooperate with vehicle manufactures in the planning of constructing a station along the highway, or directly cooperate with potential customers (e.g., hauliers), when constructing stations in urban locations.

5 Managerial implications and conclusions

Although hydrogen refueling stations have been techno-economically assessed, and models for planning their configuration have been developed by recent research, no study has adequately and systematically evaluated the effects of refueling event patterns on the investment evaluation. To close this research gap, this study developed a novel methodological approach that couples a thermodynamic simulation and a mixed-integer optimization model. The developed thermodynamic model allows to continuously simulate complete days and, thus, to technically evaluate the effects of continuous refueling. The developed optimization model allows to systematically investigate different investment strategies for the configuration planning problem. In combination, the new approach represents a useful tool to potential operators, and can be replicated for real-world use cases and/or added to existing planning tools.

Furthermore, this study applied the novel method to a comprehensive case study that represents a pipeline-supplied 700 bar gaseous hydrogen heavy-duty truck refueling station. The effects of refueling pattern events on the investment evaluation were investigated by comparing the novel method to a reference method adapted from existing literature. It was found that the main effects and trade-offs can be modeled with both approaches, but there is a systematic difference between the more detailed and the existing method, which might lead to differently chosen configurations. Thus, a real-world planner could first use the existing method for draft planning and then adapt the novel, more detailed method for fine planning. This detailed model offers the possibility for carrying out additional analyses that require continuous modeling of refueling events, but is computationally more expensive. To this end, future research could also develop new methods to simulate the considered thermodynamic effects computationally more efficiently (e.g, using artificial neural networks) to extend the scope of possible case studies.

The results of this research's case study indicate a trade-off in compressor capacity between demand under-fulfillment and the initial investment outlay. The demand

under-fulfillment effect is found to be more significant than a simultaneous reduction in electricity consumption effect. The highest economical valuation lies in most scenarios with a configuration that does not fulfill the minimal technical design requirements. If these configurations are excluded, the station design with the highest economical valuation tends to have a booster-like configuration (strong compressor and small high-pressure storage). Future research should, thus, engineer a compressor with this very high throughput, and compare an actual booster concept station without a high-pressure storage to the suggested configuration. For a potential operator, the strong effect of demand under-fulfillment implies that it is worthwhile to upgrade compressor capacities over time or plan with rather high capacity requirements. Although slightly worse mean investment evaluations are found for such stations, the evaluations' variability significantly reduces, which allows for a more predictable planning.

It was found that investment postponement significantly increases the investment valuation. This finding is consistent with Zhao and Liu (2023). However, such postponements might have implications on other supply chain stakeholders and, in turn, on the operator. A delay in infrastructure ramp-up might delay the vehicle market ramp-up, which again is an input parameter to the capacity planning of the infrastructure operator (chicken-egg problem). These feedback loops were not investigated in this study. Thus, future research could adapt our model accordingly. The postponement might also increase the likelihood of competitors entering the market first, which also influences the demand forecast of the operator. Future research should investigate these dynamics. The postponement might also negatively effect upstream supply chain stages because it causes planning uncertainty for the companies involved in hydrogen production and transport. The postponement is also critical to political targets, because the alternative fuel infrastructure regulation requires a comprehensive hydrogen refueling network already by 2030 (European Council 2023), which is earlier than the optimal investment period in some of the scenarios presented in this studies. To prevent these negative implications on the political objective and other supply chain stakeholders, policy maker, such as the European Union, should take appropriate measures. Measures could include time-restricted subsidies that offer operators incentives to invest earlier. All findings from the optimization of the investment timing in this study are based on the assumption of a finite planning horizon, which might cause end-of-horizon effects. Potential future upgrades to the model might, therefore, include the consideration of a residual liquidation value of the investment and the analyses on the effects of planning periods of different lengths on the optimal investment strategy.

The robustness analysis in this study indicates that configuration decisions appear rather robust across demand scenarios, particularly with high back-to-back capability requirements. This means that decisions perform quite well even if the investment decision was planned based on a different scenario. This finding significantly benefits potential operators as predictions on future demand might be highly uncertain. With a min-max regret approach, the operator's planning should be based on a medium demand scenario. To further support planning under uncertainty, future research could develop a robust planning model and investigate the effects of back-to-back refueling on robust decision making. Alternatively, the existing determin-

istic model could be used by planners in a rolling horizon approach, particularly because the results in this study have shown the benefit of an investment timing delay. Updated information on the vehicle market will be available at the postponed time of investment. A rolling horizon-like approach has also been suggested by Forsberg and Karlström (2007).

The sensitivity analysis indicates a high sensitivity of the results to the demand, the assumed sales margin, and the initial investment outlay. This finding suggests a high priority for potential measures such as cooperation with customers and component suppliers. Component suppliers could focus their attention on the development and pricing of high-throughput compressors. Policy makers could focus potential incentive mechanism around the sales margin to encourage the development of a refueling station network, as envisaged in the proposed regulations. Note that the case study basis setting is rather optimistic with regard to the demand but rather pessimistic with regard to the initial investment outlays for the components (see e.g., Otto et al. (2024)). With this setting, most of the considered configurations have negative mean net present values in the medium demand scenario. It was also found that no investment has a positive evaluation when a suction pressure similar to a local distribution pipeline and medium demand are assumed. Thus, pipeline-supplied 700 bar refueling stations should be built on locations with a connection to a high pressure level pipeline, preferably with at least 50 bar, and will likely require substantial subsidies, particularly in the beginning. This finding is consistent with Otto et al. (2024), who conclude that gaseous 700 bar hydrogen refueling is the most expensive concept for heavy-duty truck hydrogen refueling and still has relatively low technological readiness. As 700 bar refueling is, at the same time, seen as the predominate future technology for hydrogen refueling for long-haul trucking (European Commission 2025), policy makers and industry planners need to consider the connection of such refueling stations during the pipeline design phase and investigate alternatives to pipeline supply.

The findings of this study are based on a number of assumptions such as homogeneous refuelings and an equal distribution of vehicle arrival times over the hour. Additionally, a set of fix economical and technical parameters is assumed. Thus, future research should systematically analyze the effects of varying additional technical parameters such as ambient temperature, number of dispensers, as well as nominal working pressure and size of individual high-pressure storage banks. Additionally, a detailed method for modeling random arrival times or initial states of charge could be incorporated to overcome these limitations.

Appendix A: Details of the thermodynamic model

In the following, details about the basic modeling approach and the specific component models used in this study are given. The individual components of the system model are based on 0D and 1D methods. This allows the transient simulation of dynamic physical systems with a short computational time. Typically, dynamic balance equations for mass and energy are used, while steady-state for the momentum balance is assumed. These balance equations are used to solve for the state vari-

ables, such as pressure, specific enthalpy (or temperature), or density, as described in detail in Richter (2008). For 0D models, the state variables are assumed to be homogeneous over the component and therefore averaged over a single control volume. For 1D models, a spatial distribution of the state variables is taken into account. For these models, the balance equations are discretized in one spatial direction using the finite volume method. The one-dimensional discretization is usually along the flow direction of the fluid, e.g. in a tube, or through a wall. Since pressures of up to 1000 bar can be reached at a hydrogen refueling station, hydrogen cannot be treated as an ideal gas, but real gas effects must be considered, as shown by Striednig et al. (2014). Thus, to calculate the thermophysical properties of hydrogen, the Helmholtz energy equation of state of Leachman et al. (2009) for normal hydrogen is used, as provided by TILMedia. For solids, constant thermophysical properties are assumed.

The control strategy for the high-pressure banks is implemented in the control unit submodel using a state machine (Otter et al. 2009). The control unit turns the compressor and precooling unit on and off, and opens and closes the relevant valves depending on the current state of the refueling and/or recovery process.

The hydrogen compressor filling the buffer banks is a simple efficiency-based model. It has a constant hydrogen throughput $\dot{m}_{\mathrm{comp}}$ when on and zero throughput when off. The compressor power demand is calculated based on the isentropic power P_{isen} for compression from low (LP) to high pressure (HP) and additionally considers an effective isentropic efficiency $\eta_{\mathrm{is,eff}}$ and electric efficiency η_{el} for the compressor and its drive:

$$P_{\mathrm{comp}} = \frac{P_{\mathrm{isen}}}{\eta_{\mathrm{is,eff}}\eta_{\mathrm{el}}} \quad \text{with} \quad P_{\mathrm{isen}} = \dot{m}_{\mathrm{comp}}\left(h_{\mathrm{HP,isen}}\left(p_{\mathrm{HP}}, s_{\mathrm{LP}}\right) - h_{\mathrm{LP}}\right). \quad \text{(A1)}$$

Here, h_{LP} is the specific enthalpy of hydrogen on the low pressure side and $h_{\mathrm{HP,isen}}\left(p_{\mathrm{HP}}, s_{\mathrm{LP}}\right)$ is the specific enthalpy of hydrogen at the high pressure side for the theoretical case of isentropic compression. The latter one is calculated by TILMedia from the high-pressure, p_{HP}, and the specific entropy at the low pressure side, s_{LP}. Cooling of the hydrogen after compression is not explicitly considered. It is assumed that the hydrogen leaves the compressor with a temperature 15 K above ambient and the corresponding energy demand for cooling is included in the compressor efficiency. A single high-pressure bank typically consists of several tanks in parallel. Similar to the vehicle, the behavior of individual tanks of the high-pressure banks is not relevant for this study. Therefore, the model considers only one effective volume per bank, which is assumed to always be at ambient temperature, i.e., to be isothermal. For the precooling unit an efficiency-based model is used, similar to the model from Bauer et al. (2019). The cooling heat flow rate to be extracted from the hydrogen is given by

$$\dot{Q}_{\mathrm{precooling}} = \dot{m}_{\mathrm{refueling}}\left(h_{\mathrm{in}} - h_{\mathrm{out}}\left(p_{\mathrm{in}}, T_{\mathrm{precooling}}\right)\right). \quad \text{(A2)}$$

Here, $\left(\dot{m}_{\mathrm{refueling}}\right)$ is the hydrogen refueling mass flow rate transferred to the vehicle, $\left(h_{\mathrm{in}}\right)$ is the specific enthalpy of hydrogen at the inlet of the precooling

unit, and $h_{\text{out}}\left(p_{\text{in}}, T_{\text{precooling}}\right)$ is the specific enthalpy of hydrogen at the outlet of the precooling unit. The specific enthalpy at the outlet is calculated using the desired precooling temperature $T_{\text{precooling}}$ and assuming no pressure drop in the heat exchanger, i.e., $p_{\text{out}} = p_{\text{in}}$. The energy demand for the precooling unit is then calculated by

$$P_{\text{precooling}} = \frac{\dot{Q}_{\text{precooling}}}{\eta_{\text{precooling}} COP_{\text{Carnot}}} \quad \text{with} \quad COP_{\text{Carnot}} = \frac{T_{\text{precooling}}}{T_{\text{ambient}} - T_{\text{precooling}}}. \tag{A3}$$

Here, COP_{Carnot} is the Carnot efficiency, which is the theoretical efficiency of an ideal refrigeration cycle, and $\eta_{\text{precooling}}$ is the relative efficiency of the real precooling unit. In practice, each precooling unit has a lower and upper limit for the cooling capacity. Thus, it has to be dimensioned to match the anticipated use cases of the refueling station. For the sake of simplicity of this study, it is assumed that the precooling unit is perfectly matched to the application being studied, i.e., there is no relevant upper or lower limit to the cooling capacity, and the desired precooling temperature can always be achieved. For the vehicle tanks a detailed model is used based the model developed in the HyTransfer Project (CORDIS (Publications Office of the European Union) 2017; Bourgeois et al. 2017). It consists of a zero-dimensional gas volume, i.e. ideal mixing inside the tank is assumed, and two wall layers representing the liner and wrapping of Type III and Type IV tanks. Each wall layer can be discretized in one dimension through the thickness in order to capture the transient temperature distribution through these layers during filling and emptying. The consideration of these effects is particularly relevant for the investigation and development of new tank protocols in order to find the maximum allowed refueling speed without overheating of the vehicle tanks. For the heat transfer between the hydrogen inside the tank and the liner (inner wall layer) and between the wrapping (outer wall layer) and the ambient, constant heat transfer coefficients are used. Lastly, the valves are modeled using the Saint-Venant and Wantzel equation. For the on-tank valve, nozzle, and receptacle typical flow coefficients (C_{V}) are assumed in order to estimate the pressure drop between the hydrogen refueling station and the vehicle tanks. On-tank valve and receptacle are assumed to be always open, while the nozzle is only open during a refueling process. The valves at the inlets and outlets of the high-pressure banks open and close depending on the respective bank being filled and/or emptied. When open, the flow coefficients are set to a large value, so pressure drops are negligible.

Appendix B: Database

Table 3 Overview over the data used in this study

Parameter		Value	Source	Explanation
Compressor				
Initial Investment Outlay	$cf_c^{\text{constr.}}$	$51,901\ \$_{2015} \cdot TP^{0.65}$	Mayer et al. (2019) based on Pratt et al. (2015)	TP = throughput @20 bar suction pressure = throughput @ 80 bar/throughput factor
Throughput Factor		4	Calculated from El-gowainy et al. (2014)	
Lifetime	$ls^{\text{comp.}}$	10 years	Parks et al. (2020)	
Maintenance Rate	$f^{\text{maint., comp.}}$	8%	Mayer et al. (2019)	2015 value
High-Pressure Storage				
Initial Investment Outlay	$cf_s^{\text{constr.}}$	$343.06\ €_{2015} \cdot e^{0.02005 \cdot p} \cdot m$	Modified from Mayer et al. (2019)	p = max. storage pressure in MPa @ 20°C; m = mass in kg @ 20°C and 95 MPa; applied to 95 MPa, but 90 MPa in Mayer et al. (2019)
Lifetime	$ls^{\text{stor.}}$	20 years	Mayer et al. (2019)	
Maintenance Rate	$f^{\text{maint., stor.}}$	3.5%	Mayer et al. (2019)	
Additional Components				
Initial Investment Outlay	cf^{other}	500,000 €	Own assumption based on Mayer et al. (2019)	
Maintenance Rate	$f^{\text{maint., other}}$	2%	Mayer et al. (2019) based on Nistor et al. (2016)	Value for "several components"
Economic				
Discount Rate	h	6%	Own assumption based on Mayer et al. (2019)	Rounded to the integer
Surplus on Investment	$f^{\text{surp.}}$	53%	Calculated from Parks et al. (2020)	
Net Margin on Hydrogen	cf^{H2}	2.5 €/kg$_{\text{H2}}$	Own assumption	About equal "mid-level scenario 2030" in Zhou and Searle (2022)
Purchase Price of Electricity	cf^{ele}	0.15 €/kWh	Own assumption based on Destatis (2024)	
Monetary Value		$€_{2024}$		
Exchange Rate		1.08	Federal Bank of Germany (2024)	€ to $ in 2024

Table 3 (continued)

Economic

Deflator		1.31	OECD (2024)	Gross domestic product, market prices, deflator Germany (2015 value/2024 value)
Market Share (S-Curve)		$A + \dfrac{K - A}{(C + e^{-B(t-M)})^{1/\nu}}$		
	A	0	Own assumption	Initial market share
	B	0.3	Forsberg and Karlström (2007)	Growth rate
	C	1	Own assumption	
	ν	1	Own assumption	
	M	10	Own assumption	Time of maximum growth rate with $\nu = 1$
	K	Varied between 2.5 and 50 vehicles/day		Upper asymptote/maximum market share

Waiting Line and General Thermodynamic Model

Maximum Line length		1	Own assumption	
Maximum Waiting Time		45 min	Own assumption	Duration of the mandatory driving break for truck drivers in the EU
Handling Time		5 min	Own assumption based on Genovese et al. (2021)	
Vehicle Hydrogen Storage Capacity		80 kg	Otto et al. (2024)	
Average Pressure Ramp Rate		7.75 MPa/min	Ludwig-Bölkow-Systemtechnik GmbH (2023)	Approx. 10 min refueling time
Ambient Temperature	T_{ambient}	10 °C	Mayer et al. (2019)	Average Ambient Temperature in Germany
Initial Vehicle Pressure		50 bar	Own assumption	
Target State of Charge		95 %	Own assumption based on SAE International (2024)	
H_2-Compressor Effective Isentropic efficiency	$\eta_{\mathrm{is,eff}}$	0.73	Bauer et al. (2019)	

Waiting Line and General Thermodynamic Model			
H$_2$-Compressor Electric Efficiency	η_{el}	0.93	Bauer et al. (2019)
Relative Efficiency of Precooling Unit	$\eta_{precooling}$	0.28	Estimated from Elgowainy et al. (2017)
Precooling Temperature	$T_{precooling}$	$-20\,°C$	Ludwig-Bölkow-Systemtechnik GmbH (2023)

Data availability Data available upon reasonable request from the authors.

Declarations

Conflict of interest None.

References

Al-Sharafi A, Al-Buraiki A-S, Al-Sulaiman F, Antar M-A (2024) Hydrogen refueling stations powered by hybrid PV/wind renewable energy systems: Techno-socio-economic assessment. Energy Convers Manag X22. https://doi.org/10.1016/j.ecmx.2024.100584

Barthelemy H, Weber M, Barbier F (2017) Hydrogen storage: recent improvements and industrial perspectives. Int J Hydrogen Energy 42(11):7254–7262. https://doi.org/10.1016/j.ijhydene.2016.03.178

Bauer A, Mayer T, Semmel M, Guerrero Morales M-A, Wind J (2019) Energetic evaluation of hydrogen refueling stations with liquid or gaseous stored hydrogen. Int J Hydrogen Energy 44(13):6795–6812. https://doi.org/10.1016/j.ijhydene.2019.01.087

Blazquez-Diaz C (2019) Techno-economic modelling and analysis of hydrogen fuelling stations. Int J Hydrogen Energy 44(2):495–510. https://doi.org/10.1016/j.ijhydene.2018.11.001

Bourgeois T, Brachmann T, Barth F, Ammouri F, Baraldi D, Melideo D, Lemonnier D (2017) Optimization of hydrogen vehicle refuelling requirements. Int J Hydrogen Energy 42(19):13789–13809. https://doi.org/10.1016/j.ijhydene.2017.01.165

Brown T, Stephens-Romero S, Scott Samuelsen G (2012) Quantitative analysis of a successful public hydrogen station. Int J Hydrogen Energy 37(17):12731–12740. https://doi.org/10.1016/j.ijhydene.2012.06.008

Caponi R, Bocci E, Del Zotto L (2022) Techno-economic model for scaling up of hydrogen refueling stations. Energies 15(20):1–16. https://doi.org/10.3390/en15207518

Caponi R, Ferrario A-M, Bocci E, Bødker S, del Zotto L (2022) Single-tank storage versus multi-tank cascade system in hydrogen refueling stations for fuel cell buses. Int J Hydrogen Energy 47(64):27633–27645. https://doi.org/10.1016/j.ijhydene.2022.06.100

CORDIS (Publications Office of the European Union) (2017) Pre-Normative Research for Thermody-namic Optimization of Fast Hydrogen Transfer | HYTRANSFER Project | Fact Sheet | FP7. Retrieved 2024-05-06 from https://cordis.europa.eu/project/id/325277

Dassault Systèmes. (2023) Dymola–Dynamic Modeling Laboratory. Dassault Systèmes. Retrieved 2024-01-05 from https://www.3ds.com/products/catia/dymola

De Miguel N, Acosta Iborra B, Baraldi D, Melideo R, Ortiz Cebolla R, Moretto P (2016) The role of initial tank temperature on refuelling of on-board hydrogen tanks. Int J Hydrogen Energy 41(20):8606–8615. https://doi.org/10.1016/j.ijhydene.2016.03.158

Destatis. (2024) Average Natural Gas and Electricity Prices [in German only]. Retrieved 2025-01-20 from https://www.destatis.de/DE/Themen/Wirtschaft/Preise/Erdgas-Strom-DurchschnittsPreise/_inhalt.html#421260

DIN e.V. (2020) Monetary valuation of environmental impacts and related environmental aspects (EN ISO 14008:2020)

Elgowainy A, Mintz M, Kelly B, Hooks M, Paster M (2008) Optimization of compression and storage requirements at hydrogen refueling stations. In: ASME 2008 pressure vessels and piping conference. American Society of Mechanical Engineers. pp 131–136

Elgowainy A, Reddi K, Lee D-Y, Rustagi N, Gupta E (2017) Techno-economic and thermodynamic analysis of pre-cooling systems at gaseous hydrogen refueling stations. Int J Hydrogen Energy 42(49):29067–29079. https://doi.org/10.1016/j.ijhydene.2017.09.087

Elgowainy A, Reddi K, Sutherland E, Joseck F (2014) Tube-trailer consolidation strategy for reducing hydrogen refueling station costs. Int J Hydrogen Energy 39(35):20197–20206. https://doi.org/10.1016/j.ijhydene.2014.10.030

European Commission: Directorate-General for Mobility and Transport, Ramboll, Transport & Mobil-ity, University of Antwerp (2025) Market readiness analysis—Expected uptake of alternative fuel heavy-duty vehicles until 2030 and their corresponding infrastructure needs. Publications Office of the European Unio. https://doi.org/10.2832/4625934

European Council (2023) Alternative fuels infrastructure: Council adopts new law for more recharging and refuelling stations across Europe. Retrieved 2023-09-26 from https://www.consilium.europa.eu/en/press/press-releases/2023/07/25/alternative-fuels-infrastructure-council-adopts-new-law-for-more-recharging-and-refuelling-stations-across-europe/:~:text=The%20alternative%20fuels%20infrastructure%20regulation,achieve%20climate%20neutrality%20in%202050

Feder Highway Research Institute. (2022) Automatic permanent counting stations on highways and main roads [in German only]. Retrieved 2025-01-08 from https://www.bast.de/DE/Verkehrstechnik/Fachthemen/v2-verkehrszaehlung/Verkehrszaehlung.html?nn=1817946

Federal Bank of Germany. (2024) Bundesbank in-house exchange rate. Retrieved 2025-01-15 from https://www.bundesbank.de/en/statistics/time-series-databases

Forsberg P, Karlström M (2007) On optimal investment strategies for a hydrogen refueling station. Int J Hydrogen Energy 32(5):647–660. https://doi.org/10.1016/j.ijhydene.2006.05.018

Genovese M, Blekhman D, Dray M, Fragiacomo P (2021) Hydrogen station in situ back-to-back fueling data for design and modeling. J Clean Prod 329 https://doi.org/10.1016/j.jclepro.2021.129737

Götze U, Northcott D, Schuster P (2015) Investment Appraisal. Berlin Heidelberg Springer Berlin Heidel-berg. https://doi.org/10.1007/978-3-662-45851-8

Grüger F, Dylewski L, Robinius M, Stolten D (2018) Carsharing with fuel cell vehicles: Sizing hydrogen refueling stations based on refueling behavior. Appl Energy 228:1540–1549. https://doi.org/10.1016/j.apenergy.2018.07.014

H2 Mobility. (2010) 70 MPa Hydrogen Refuelling Station Standardization—Functional Description of Station Modules. (Tech. Rep.)

Hindmarsh A-C, Brown P-N, Grant K-E, Lee S-L, Serban R, Shumaker D-E, Woodward C-S (2005) SUNDIALS: Suite of nonlinear and differential/algebraic equation solvers. ACM Trans Math Softw 31(3):363–396. https://doi.org/10.1145/1089014.1089020

Ku A-Y, Reddi K, Elgowainy A, McRobie J, Li J (2022) Liquid pump-enabled hydrogen refueling system for medium and heavy duty fuel cell vehicles: station design and technoeconomic assessment. Int J Hydrogen Energy 47(61):25486–25498. https://doi.org/10.1016/j.ijhydene.2022.05.283

Kuroki T, Nagasawa K, Peters M, Leighton D, Kurtz J, Sakoda N, Takata Y (2021) Thermodynamic mod-eling of hydrogen fueling process from high-pressure storage tank to vehicle tank. Int J Hydrogen Energy 46(42):22004–22017. https://doi.org/10.1016/j.ijhydene.2021.04.037

Kuroki T, Sakoda N, Shinzato K, Monde M, Takata Y (2018) Dynamic simulation for optimal hydrogen refueling method to Fuel Cell Vehicle tanks. Int J Hydrogen Energy 43(11):5714–5721. https://doi.org/10.1016/j.ijhydene.2018.01.111

Kurtz J, Bradley T, Winkler E, Gearhart C (2020) Predicting demand for hydrogen station fueling. Int J Hydrogen Energy 45(56):32298–32310. https://doi.org/10.1016/j.ijhydene.2019.10.014

Leachman J-W, Jacobsen R-T, Penoncello S-G, Lemmon E-W (2009) Fundamental equations of state for parahydrogen, normal hydrogen, and orthohydrogen. J Phys Chem Ref Data 38(3):721–748. https://doi.org/10.1063/1.3160306

Ludwig-Bölkow-Systemtechnik GmbH (2023) PRHYDE - Protocol for Heavy-Duty Hydrogen Refuelling. Retrieved 2024-03-28 from https://lbst.de/prhyde/

Luss H (1982) Operations research and capacity expansion problems: a survey. Oper Res 30(5):907–947

Martínez-Costa C, Mas-Machuca M, Benedito E, Corominas A (2014) A review of mathematical programming models for strategic capacity planning in manufacturing. Int J Prod Econ 153:66–85. https://doi.org/10.1016/j.ijpe.2014.03.011

Mayer T, Semmel M, Guerrero Morales M-A, Schmidt K-M, Bauer A, Wind J (2019) Techno-economic evaluation of hydrogen refueling stations with liquid or gaseous stored hydrogen. Int J Hydrogen Energy 44(47):25809–25833. https://doi.org/10.1016/j.ijhydene.2019.08.051

Mintz M, Elgowainy A, Gardiner M (2009) Rethinking hydrogen fueling: Insights from delivery modeling. Transp Res Rec 2139:46–54. https://doi.org/10.3141/2139-06

Modelica Association. (2023) Modelica—A Unified Object-Oriented Language for Systems Modeling: Language Specifications Version 3.6. Modelica Association. Retrieved 2024-01-05 from https://specification.modelica.org/maint/3.6/MLS.pdf

Modelica Association (2024) Functional Mock-up Interface. Retrieved 2024-12-28 from https://fmi-standard.org/

Nistor S, Dave S, Fan Z, Sooriyabandara M (2016) Technical and economic analysis of hydrogen refuelling. Appl Energy 167:211–220. https://doi.org/10.1016/j.apenergy.2015.10.094

NOW GmbH (2024) Versorgung der H2-Tankstelleninfrastruktur in Deutschland über ein H2-Pipeline-Netz (Tech. Rep.)

OECD. (2024) Economic Outlook 115 (Gross domestic product, market prices, deflator). Retrieved 2025-01-05 from https://data-explorer.oecd.org/vis?tm=gdp%20deflator&pg=0 &snb=22 &vw=tb &df%5Bds%5D=dsDisseminateFinalDMZ &df%5Bid%5D=DSD_EO%40DF_EO &df%5Bag%5D=OECD.ECO.MAD &df%5Bvs%5D=1.1 &dq=.PGDP.A &pd=2000%2C &to%5BTIME_PERIOD%5D=false

Otter M, Malmheden M, Elmqvist H, Mattsson S-E, Johnsson C (2009) A New Formalism for Modeling of Reactive and Hybrid Systems. The 7 International Modelica Conference, Como, Italy, pp 364–377. https://doi.org/10.3384/ecp09430108

Otto T, Erhart P, Kraus S, Grube T, Linßen J, Stolten D (2024) Comparing hydrogen refueling concepts for heavy-duty vehicles. Int J Hydrogen Energy 110:115–127. https://doi.org/10.1016/j.ijhydene.2025.01.498

Parks G, Boyd R, Cornish J, Remick R (2020) Hydrogen station compression, storage, and dispensing technical status and costs (Tech. Rep.)

Pratt J, Terlip D, Ainscough C, Kurtz J, Elgowainy A (2015) H2FIRST reference station design task: project deliverable 2-2 (Tech. Rep.)

Reddi K, Elgowainy A, Rustagi N, Gupta E (2017) Impact of hydrogen refueling configurations and market parameters on the refueling cost of hydrogen. Int J Hydrogen Energy 42(34):21855–21865. https://doi.org/10.1016/j.ijhydene.2017.05.122

Reddi K, Elgowainy A, Sutherland E (2014) Hydrogen refueling station compression and storage optimization with tube-trailer deliveries. Int J Hydrogen Energy 39(33):19169–19181. https://doi.org/10.1016/j.ijhydene.2014.09.099

Richter C (2008) Proposal of New Object-Oriented Equation-Based Model Libraries for Thermodynamic SystemsBraunschweigTechnische Universität Carolo-Wilhelmina zu Braunschweig. https://doi.org/10.24355/DBBS.084-200806100200-3

Rothuizen E, Rokni M (2014) Optimization of the overall energy consumption in cascade fueling stations for hydrogen vehicles. Int J Hydrogen Energy 39(1):582–592. https://doi.org/10.1016/j.ijhydene.2013.10.066

SAE International (2020) J2601—Fueling Protocols for Light Duty Gaseous Hydrogen Surface Vehicles (Tech. Rep.)

SAE International (2024) J2601-5—High-Flow Prescriptive Fueling Protocols for Gaseous Hydrogen Powered Medium and Heavy-Duty Vehicles (Tech. Rep.)

Short W, Packey D, Holt T (1995) A manual for the economic evaluation of energy efficiency and renewable energy technologies (Tech. Rep.). Golden, CONational Renewable Energy Laboratory (NREL) https://doi.org/10.2172/35391

Šimunović J, Pivac I, Barbir F (2022) Techno-economic assessment of hydrogen refueling station: a case study in Croatia. Int J Hydrogen Energy 47(57):24155–24168. https://doi.org/10.1016/j.ijhydene.2022.05.278

Sprik S, Murphy D, Kuroki T, Terlip D, Eichman J, Penev M, Kurtz J (2018) Hydrogen Station Capacity Evaluation. Tech Rep

Striednig M, Brandstätter S, Sartory M, Klell M (2014) Thermodynamic real gas analysis of a tank filling process. Int J Hydrogen Energy 39(16):8495–8509. https://doi.org/10.1016/j.ijhydene.2014.03.028

Sun J, Peng Y, Lu D, Chen X, Xu W, Weng L, Wu J (2022) Optimized configuration and operating plan for hydrogen refueling station with on-site electrolytic production. Energies 15(7). https://doi.org/10.3390/en15072348

Talpacci E, Reuβ, M, Grube T, Cilibrizzi P, Gunnella R, Robinius M, Stolten D (2018) Effect of cascade storage system topology on the cooling energy consumption in fueling stations for hydrogen vehicles. Int J Hydrogen Energy 43(12):6256–6265. https://doi.org/10.1016/j.ijhydene.2018.02.030

Tian Z, Lv H, Zhou W, Zhang C, He P (2022) Review on equipment configuration and operation process optimization of hydrogen refueling station. Int J Hydrogen Energy 47(5):3033–3053. https://doi.org/10.1016/j.ijhydene.2021.10.238

TLK-Thermo GmbH. (2024a) Simulator Suite. Retrieved 2024-12-28 from https://www.tlk-thermo.com/en/software/simulator-suite

TLK-Thermo GmbH. (2024b) TIL Suite 3.16.0. TLK-Thermo GmbH. Braunschweig. Retrieved 2024-08-20 from https://www.tlk-thermo.de/en/software/til-suite

UL Solutions. (2024) Homer Energy. Retrieved 2025-01-15 from https://www.homerenergy.com

Zhao T, Liu Z (2023) Investment timing analysis of hydrogen-refueling stations and the case of china: independent or co-operative investment? Energies 16(13). https://doi.org/10.3390/en16135032

Zhao T, Liu Z (2024) Investment of hydrogen refueling station based on compound real options. Int J Hydrogen Energy 57:198–209. https://doi.org/10.1016/j.ijhydene.2024.01.040

Zhou Y, Searle S (2022) Cost of renewable hydrogen produced onsite at hydrogen refueling stations in Europe (Tech.Rep)

Authors and Affiliations

Tjard Bätge[1] · **Steffen Heinke[2]** · **Christian Weckenborg[3]** · **Marco Karig[1]** · **Wilhelm Tegethoff[2]** · **Jürgen Köhler[2]** · **Thomas S. Spengler[1]**

✉ Tjard Bätge
t.baetge@tu-braunschweig.de

[1] Institute of Automotive Management and Industrial Production, Technische Universität Braunschweig, Mühlenpfordtstr. 23, 38106 Braunschweig, Germany

[2] Institut für Thermodynamik, Technische Universität Braunschweig, Hans-Sommer-Straße 5, 38106 Braunschweig, Germany

[3] University of Regensburg, Universitätsstraße 31, 93053 Regensburg, Germany